

The role of fractalkine – CX3CR1 signaling in the development of obesity

Ph.D dissertation

Ágnes Polyák



Pázmány Péter Catholic University

Faculty of Information Technology and Bionics

Roska Tamás Doctoral School of Sciences and Technology

Supervisor: Dr. Krisztina Kovács

Budapest, 2017

Table of Contents

1. Abbreviations	4
2. Introduction	7
2.1. The obesity epidemic.....	7
2.2. Energy homeostasis	7
2.3. Types of adipose tissue.....	9
2.4. Obesity related macrophage accumulation and inflammation.....	11
2.5. Chemokines and the fractalkine-CX3CR1 system	15
3. Aims	20
4. Materials and methods.....	21
4.1. Animals and diet.....	21
4.2. Experimental design	22
4.3. Body composition analysis.....	22
4.4. Glucose tolerance test.....	23
4.5. Hormone and cytokine measurements.....	23
4.6. Histology and quantitative analysis	23
4.7. Immunohistochemistry	24
4.8. Core body temperature measurement and cold challenge	24
4.9. Gene expression analysis by quantitative real-time PCR	25
4.10. Primer design.....	25
4.11. Normalized <i>Gfp</i> expression	27
4.12. Western blot analysis.....	27
4.13. Stromal Vascular Fraction preparation and Flow Cytometry	28
4.14. Statistical analysis.....	28
5. Results	29
5.1. Fractalkine – CX3CR1 signaling is necessary for the development of the characteristics of obesity	29
5.1.1. Body weight gain, body fat gain.....	29
5.1.2. Fat depots.....	30
5.1.3. Glucose intolerance	32
5.1.4. Cold tolerance.....	33
5.1.5. Elevated plasma cytokine concentrations	34
5.1.6. Hypothalamo-pituitary-adrenocortical (HPA) axis	35
5.2. Fractalkine – CX3CR1 signaling dependent adipose tissue remodeling.....	36

5.3.	Accumulation of macrophages to adipose tissues is fractalkine – CX3CR1 signaling dependent.....	37
5.3.1.	F4/80 Immunohistochemistry.....	38
5.3.2.	Gfp mRNA expression	40
5.3.3.	FACS analysis	40
5.4.	Inflammation in adipose tissues is related with the amount of macrophages.....	41
5.4.1.	Chemokine expression in adipose tissues.....	41
5.4.2.	Inflammatory cytokine expression in adipose tissues.....	42
5.5.	10 weeks of FatED does not induce severe inflammation in liver	44
5.6.	10 weeks of FatED does not induce tissue inflammation in hypothalamus	45
	Inflammatory markers and energy homeostasis regulatory peptides.....	45
5.7.	Fractalkine - CX3CR1 signaling affects lipolysis/lipogenesis balance in BAT	47
5.8.	Fractalkine – CX3CR1 signaling affects the expression of BAT thermogenic and metabolic-related markers	48
5.9.	FatED results in elevated UCP1 protein levels in fractalkine deficient mice.....	50
6.	Discussion.....	51
7.	New scientific results.....	58
	Thesis I.	58
	Thesis II.	58
	Thesis III.....	59
8.	Possible applications	60
9.	Acknowledgement.....	61
10.	References	62

1. Abbreviations

ABC	–	avidin-biotin complex
ACK	–	ammonium-chloride-potassium lysis buffer
ACTH	–	adrenocorticotrophic hormone
ADAM10	–	a disintegrin and metalloproteinase domain 10
ADAM17 (TACE)	–	a disintegrin and metalloproteinase domain 17 tumor necrosis factor, alpha, converting enzyme
ADRB3	–	adrenoceptor beta 3
AgRP	–	agouti related neuropeptide
ARC	–	arcuate nucleus
ARG1	–	arginase 1
ATGL (PNPLA2)	–	adipose triglyceride lipase
ATM	–	adipose tissue macrophages
ATP	–	adenosine triphosphate
BAT	–	brown adipose tissue
BMI	–	body mass index
CART	–	cocaine and amphetamine regulated transcript
CCL2 (MCP1)	–	chemokine (C-C motif) ligand 2; (monocyte chemotactic protein-1)
CLS	–	crown-like structures
CORT	–	corticosterone
CRH	–	corticotropin-releasing hormone
CX3CL1	–	fractalkine
CX3CR1	–	fractalkine receptor
DAB	–	3,3'-diaminobenzidine
DC	–	dendritic cell
DGAT1	–	diacylglycerol O-acyltransferase 1
DIO	–	diet induced obesity
DIO2	–	type 2 iodothyronine deiodinase
DNase	–	deoxyribonuclease
EDTA	–	ethylenediaminetetraacetic acid
EWAT	–	epididymal white adipose tissue
FA	–	fatty acid
FACS	–	fluorescence-activated cell sorting
FatED	–	fat-enriched diet

GAPDH	– glyceraldehyde 3-phosphate dehydrogenase
GFP	– green fluorescent protein
GLUT4	– glucose transporter type 4
GPAT	– glycerol-3-phosphate acyltransferase
GTT	– glucose tolerance test
H&E	– hematoxylin-eosin (staining)
HFD	– high fat diet
HRP	– horse radish peroxidase
HSD11B1 (11 β HSD1)	– 11 β -hydroxysteroid dehydrogenase type 1
HSL (LIPE)	– lipase, hormone-sensitive
IBAT	– interscapular brown adipose tissue
IFN γ	– interferon gamma
IL10	– interleukin 10
IL1A	– interleukin 1 alpha
IL1B	– interleukin 1 beta
IL6	– interleukin 6
KPBS	– potassium phosphate buffered saline
MD	– minimal disease
MGAT	– mannosyl (alpha-1,3-)-glycoprotein beta-1,2-N-acetylglucosaminyltransferase
MGL	– monoglyceride lipase
MRI	– magnetic resonance imaging
m β CD	– methyl- β -cyclodextrin
NALP3	– NACHT, LRR and PYD domains-containing protein 3
ND	– normal diet
NK cells	– natural killer cells
NLRP3	– NLR family, pyrin domain containing 3
NPY	– neuropeptide Y
PGC1A (PPARGC1A)	– peroxisome proliferator-activated receptor gamma, coactivator 1 alpha
PMA	– phorbol-12-Myristate-13-Acetate
PND	– postnatal day
POMC	– pro-opiomelanocortin
PPARG	– peroxisome proliferator-activated receptor gamma
qPCR	– quantitative real time polymerase chain reaction

RIA	– radioimmunoassay
RIPA	– radio-immunoprecipitation assay buffer
RT-PCR	– real-time polymerase chain reaction
SLO	– streptolysin O
SNS	– sympathetic nervous system
SPF	– specified pathogen free
SVF	– stromal vascular fraction
SWAT	– subcutaneous white adipose tissue
T3	– triiodothyronine
TBST	– Tris buffered saline with Tween
TH	– tyrosine hydroxylase
TNF α	– tumor necrosis factor alpha
UCP1	– uncoupling protein 1
WAT	– white adipose tissue

2. Introduction

2.1. The obesity epidemic

Overweight and obesity are defined as abnormal or excessive fat accumulation that may impair health. Worldwide obesity has more than doubled in the last 35 years. 39% of adults were overweight in 2014, and 13% were obese. Children all over the world are also affected by obesity and related complications [1]. Obesity affects all socioeconomic backgrounds and ethnicities and is a prerequisite for metabolic syndrome. Metabolic syndrome is a clustering of risk factors, such as central obesity, insulin resistance, dyslipidaemia and hypertension that together culminate in the increased risk of type 2 diabetes mellitus and cardiovascular diseases [2]. Obesity and overweight are associated with chronic low grade inflammation. This inflammatory condition plays an important part in the etiology of the metabolic syndrome and largely contributes to the related pathological outcomes [3].

Body weight can be categorized based on a person's body mass index (BMI). BMI is a person's weight in kilograms divided by the square of height in meters. It can be used for population assessment of overweight and obesity. For adults 20 years old and older, BMI is interpreted using standard weight status categories. These categories are: underweight (BMI < 18.5), normal or healthy weight (BMI 18.5 – 24.9), overweight (BMI 25.0 – 29.9), obese (BMI > 30.0) [4]. Raised body mass index (BMI) is a major risk factor for chronic diseases such as cardiovascular diseases, diabetes, musculoskeletal disorders and some cancers [1]

The mechanism of obesity development is still not fully understood, and new scientific results are very important to prevent and treat obesity.

2.2. Energy homeostasis

The fundamental cause of obesity and overweight is an energy imbalance between calories consumed and calories expended [1]. The brain is the main regulator of energy homeostasis, which controls energy intake and energy expenditure based on the signals of the internal and external environment [5-7]. Complex neuronal circuit within the hypothalamus and extrahypothalamic areas are responsible for maintaining energy homeostasis. Two distinct cell populations are present in the ARC. Orexigenic NPY/AgRP neurons and anorexigenic POMC/CART neurons are in the position to sense metabolic-related hormones and various nutrients and generate adequate autonomic and behavioral responses [8-10]. The autonomic

nervous system (which consists of two parts, the sympathetic and parasympathetic nervous systems) innervate peripheral metabolic tissues, including brown and white adipose tissue, liver, pancreas, and skeletal muscle. The the sympathetic nervous systems regulates thermogenesis and energy expenditure in BAT, lipid metabolism in WAT and glucose uptake in muscle. Sympathetic and parasympathetic nerves contribute to hepatic glucose production and pancreatic insulin secretion [11]. Summary of energy homeostasis is shown in Fig.1.

Nutrients consumed and absorbed are used as fuels for energy expenditure. Excess nutrients are stored in the form of fat in unlimited amounts in adipose tissues, and in the form of glycogen, in limited amounts in liver and muscle [12]. Components of energy expenditure are basal metabolism, physical activity and adaptive thermogenesis. Physical activity includes all voluntary movements, while basal metabolism refers to biochemical processes necessary to sustain life. Adaptive thermogenesis is the production of heat in response to environmental challenges, such as exposure to cold and alterations in diet [13].

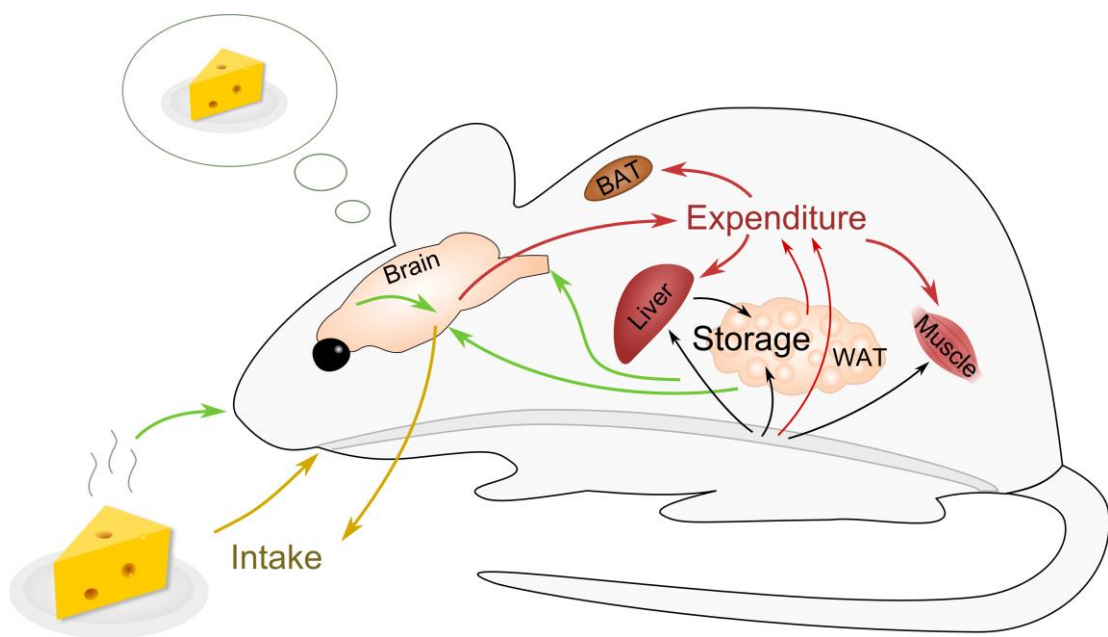


Figure 1. Components of energy homeostasis.

Brain regulates energy intake (yellow arrows) and energy expenditure (red arrows) in response to external and internal signals (green arrows). The fuels used for physical activity, basal metabolism, and adaptive thermogenesis originates from absorbed food. Excess nutrients are stored in adipose tissues, liver or muscles for further use (black arrows).

2.3. Types of adipose tissue

There are two types of adipose tissue, white and brown fat, which have distinct functions.

White adipose tissue (WAT) stores excess energy as triglycerides and displays endocrine functions by secreting adipokines and cytokines [14-16].

Brown adipose tissue (BAT) is the major site of cold-, stress- and diet-induced thermogenesis with which BAT significantly affects systemic glucose and lipid metabolism [17-19].

The distribution of fat depots in humans are shown in Fig.2.

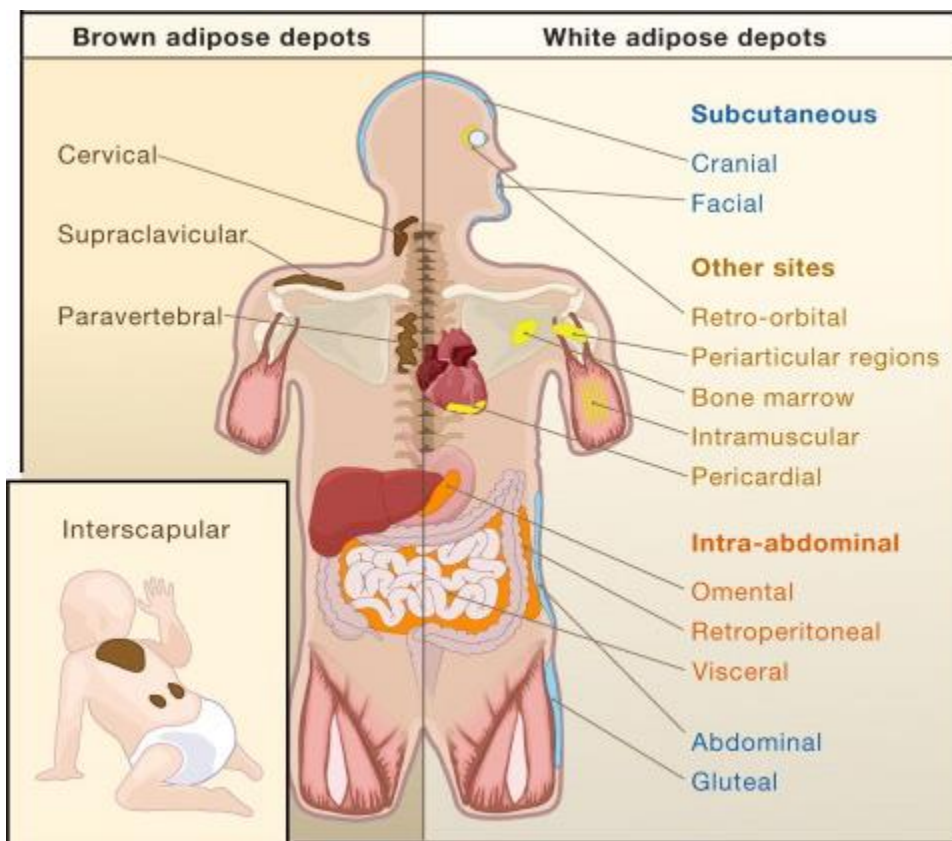


Figure 2. Fat Distribution in Human.

In human, white adipose tissue depots are found all over the body, with subcutaneous and intra-abdominal depots representing the main compartments for fat storage. Brown adipose tissue is abundant at birth and still present in adulthood but to a lesser extent. [20]

White adipocytes are spherical cells and contain one large lipid droplet. Their size mainly depends on the size of the lipid droplet stored in them. The lipid droplet consists of triglycerides and accounts for more than 90% of the cell volume. Mitochondria in white adipocytes are thin, elongated, and variable in amount [14]. Beyond the storage of excess fat,

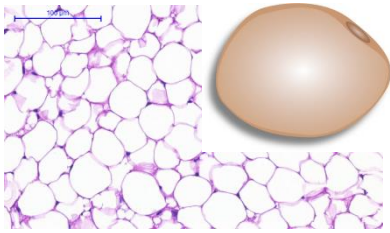
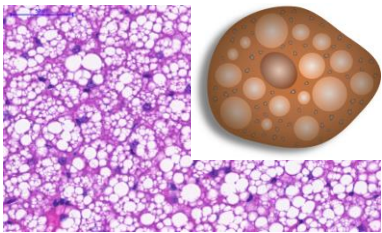
white adipocytes have important endocrine functions. With the secretion of adipokines (e.g. cytokines, leptin, adiponectin), adipocytes modulates energy homeostasis and immunity [16]. Various WAT depots might contain inducible brown-in-white (brite, beige) adipocytes. They have different origin and molecular signature from classical brown adipocytes but share the characteristics of high mitochondria content, UCP1 expression and thermogenic capacity when activated. Beige adipocyte clusters are especially prominent in the subcutaneous inguinal WAT, and develop in response to cold and certain other stimuli. Compared with brown adipocytes, beige adipocytes have more phenotypic flexibility, and can acquire a thermogenic or storage phenotype, depending on environmental cues [21-23].

Brown and beige adipocytes are multilocular and contain significantly higher number of mitochondria than other adipocytes in the body [22]. These cells are specialized to dissipate energy in the form of heat by uncoupled thermogenesis, mediated by the dissociation of mitochondrial respiratory chain electron transport from ATP synthesis via the action of uncoupling protein1 (UCP1) [15].

BAT is abundant in small mammals and in newborns and helps them to survive cold temperatures. In adults, it has long been considered to be absent, but recently several research groups demonstrated that adults have metabolically active BAT [24-28]. The amount of BAT is inversely correlated with body-mass index, especially in older people [29]. Metabolically active BAT seems to be particularly low in patients with obesity or diabetes [30]. These results suggest a significant role of brown adipose tissue in adult human metabolism and opens new opportunities to develop therapeutic interventions to treat obesity. Table 1. shows the characteristics of white and brown fat.

Both types of adipose tissues (BAT and WAT) are sensitive to environmental (temperature) - hormonal (T3, leptin, insulin, corticosteroid) - and metabolic (high fat diet) cues and display significant cellular and functional remodeling in response to these challenges.

Table 1. Comparison of white and brown fat [14].

	White fat	Brown fat
		
Function	Energy storage	Heat production
Morphology	Single lipid droplet Variable amount of mitochondria	Multiple small vacuolae Abundant mitochondria
Marker protein	Leptin	UCP1
Development	From Myf5- negative progenitor cells	From Myf5- positive progenitor cells (but there are also Myf5-negative brown fat cells which are derived from other lineages)
Human data	Large amounts are associated with increased risk of obesity-related disorders	Large amounts are associated with decreased risk of obesity-related disorders
Impact of aging	Increases with age relative to total body weight	Decreases with age

2.4. Obesity related macrophage accumulation and inflammation

In addition to adipocytes, adipose tissues contains various immune-related cells including resident macrophages (adipose tissue macrophages – ATMs), eosinophils, mast cells and T cells, which significantly contribute to their function via release of (adipo)cytokines and transmitters in paracrine or endocrine fashion [31-34]. Macrophages are present in the highest percentage in the tissue (45-55%, depending on the body weight) [35]. During the development of obesity not only the ratio of immune cells changes but also their inflammatory state. Lean adipose tissue contains various anti-inflammatory immune cells, such as eosinophils, M2 (anti-inflammatory) macrophages, type 2 T helper (Th2) cells, invariant natural killer T (iNKT) cells, and regulatory T (Treg) cells. These immune cells help maintaining normal tissue function. In obese adipose tissue, the number of proinflammatory immune cells, including neutrophils, M1 (proinflammatory) macrophages, mast cells, type 1 T helper (Th1) cells, and CD8 T cells, are greatly elevated. Simultaneously, reduced number of

anti-inflammatory immune cells accelerates proinflammatory response and adipose tissue dysfunction (Fig. 3) [36].

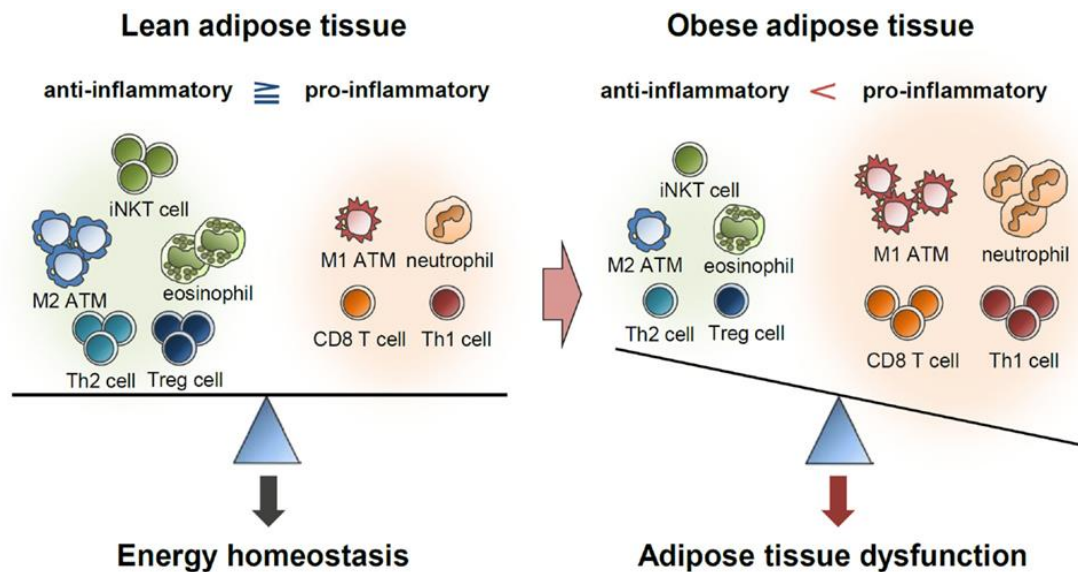


Figure 3. Balance of immune responses in the regulation of adipose tissue function.

In lean adipose tissue anti-inflammatory immune cells dominate, which help maintaining normal tissue function. In obese adipose tissue the numbers of immune cells are elevated and the number of anti-inflammatory immune cells are reduced, which leads to adipose tissue dysfunction. [36]

In the early phases of diet-induced obesity the amount of fat in adipocytes increases in visceral adipose tissue. Hypertrophic adipocytes change their hormone and chemokine expression, which leads to the increase of immune cells in the tissue. In the first days after the initiation of high fat diet, neutrophils infiltrate into the adipose tissue. After weeks, the numbers of natural killer (NK) cells and macrophages also increase. NK cells increase their number only by local proliferation. Increased number of macrophages originate from (at least) two distinct sources: local proliferation of tissue resident macrophages and/or the infiltration of monocytes from the blood [37]. Infiltrated monocytes differentiate into macrophages in the tissue [38]. Circulating monocytes originate in the bone marrow. Experiments on bone marrow transplanted mice showed that after 6 weeks on a high-fat diet, 85% of the F4/80+ cells (macrophages) in periepididymal adipose tissue of the recipient mice were donor-derived [39], which indicates that these cells migrated to the adipose tissue from the circulation.

Furthermore, in obese animals and humans the key event in the induction of adipose inflammation is the polarization of macrophages from anti-inflammatory (M2-like) to proinflammatory (M1-like) form [37, 40, 41]. M2 anti-inflammatory macrophages are

characterized – among others - by arginase 1, and IL10 expression. Diet-induced obesity decreases the expression of these genes in macrophages while increases the proinflammatory gene expression (TNF α , IL1, IL6) that are characteristic of M1 macrophages [42, 43]. Important signals to M1 polarization are interferon gamma (IFN γ) secreted by NK and T cells and pathogen-associated molecular patterns (PAMPs) from periphery. M1 polarized macrophages are sensitive to a range of proinflammatory stimuli, such as leukotrienes, danger associated molecular patterns (DAMPs) from necrotic adipocytes, and FFA-Fetuin-A complexes from the periphery. Proinflammatory cytokine expression by M1 macrophages leads to further accumulation of inflammatory immune cells and the amplification of inflammation [37]. Fig. 4. shows a summary of the development of obesity induced adipose tissue inflammation.

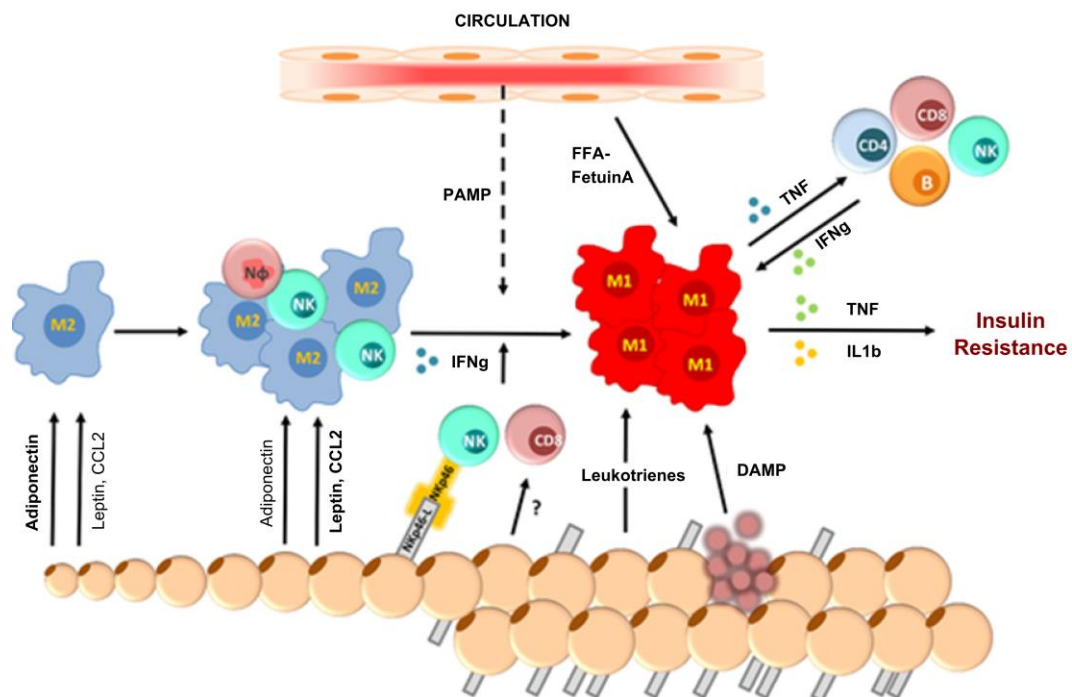


Figure 4. Model of the development of obesity-induced adipose tissue inflammation.

In response to high fat diet, adipocytes become hypertrophic and later hyperplastic, which is associated with the shift from adiponectin to leptin/CCL2 production in adipocytes and the increase in the number of immune cells in visceral WAT. As obesity persists, adipocyte stress drives CD8+ T-cell and NK-cell activation through NKp46, resulting in local production of IFN γ . Together with PAMPs coming from the periphery, this locally produced IFN γ licenses adipose tissue macrophages (ATMs) toward a proinflammatory M1 state. This makes these cells sensitive to a range of proinflammatory stimuli, such as leukotrienes, FFA-FetuinA complexes, and DAMPs from necrotic adipocytes. As a result, ATMs produce proinflammatory cytokines, such as TNF and IL1 β , and recruit more proinflammatory cells into the tissue to amplify the immune response. The chronic systemic presence of proinflammatory cytokines

derived from this response ultimately contributes to the development of insulin resistance. M1: M1 Macrophage; M2: M2 Macrophage; NΦ: Neutrophil; NK: natural killer cell [37].

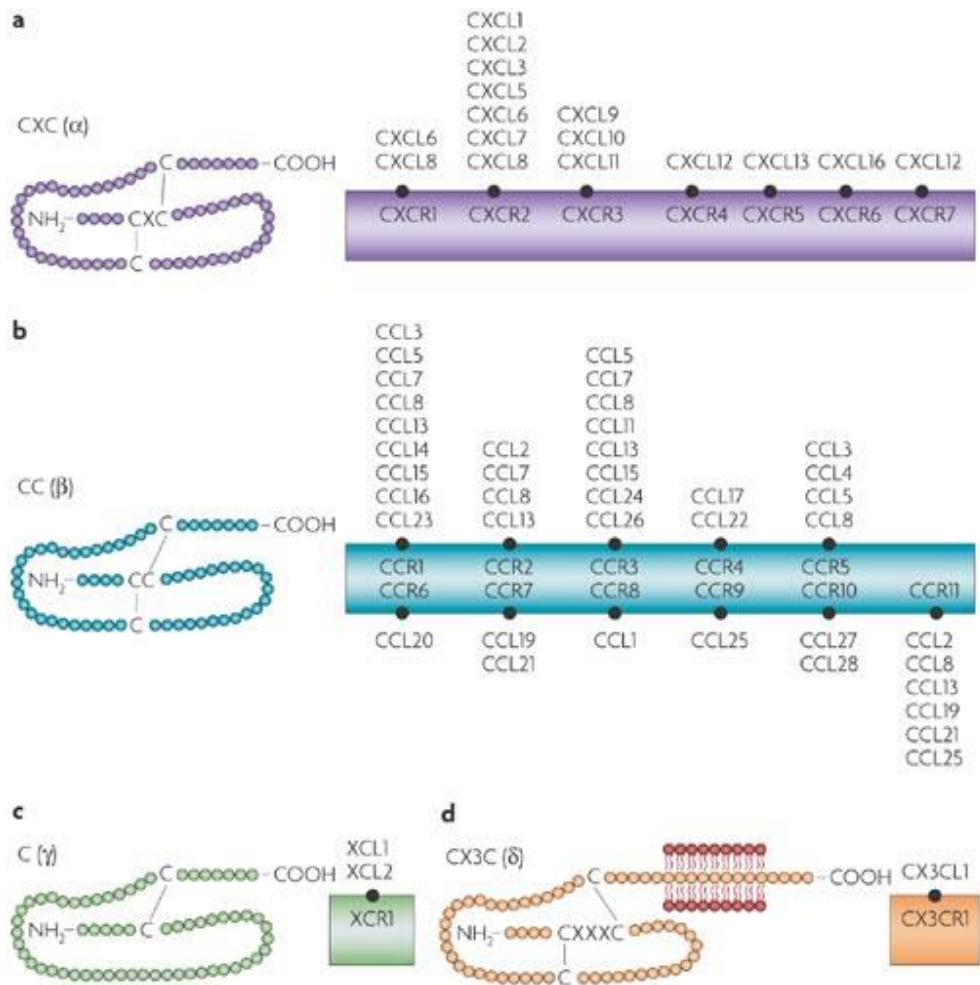
Growing evidence implicates that obesity-induced tissue inflammation is not limited to the visceral WAT but also seen in the liver and in the hypothalamus [44]. In either tissue, diet-induced inflammation is always associated with recruitment/proliferation and activation of various immune-competent cells such as monocytes, macrophages, and T cells.

However, the accumulation of macrophages to BAT, the mechanisms that recruit and activate them and their effect on thermometabolic genes has not been fully elucidated. Because these changes contribute to insulin resistance and low grade systemic metabolic inflammation which is seen in a subset of obese patients with metabolic X [45], it is important to understand the mechanisms that recruit and activate adipose tissue macrophages and the means with which local inflammation affects lipid metabolism and thermoregulation.

2.5. Chemokines and the fractalkine-CX3CR1 system

Chemokines (chemotactic cytokines) constitute the largest family of cytokines [46]. Chemokines and their receptors have an important role in trafficking of leukocytes during inflammation and immune surveillance. Furthermore they exert different functions under physiological conditions such as homeostasis, development, tissue repair, and angiogenesis but also under pathological disorders including tumorigenesis, cancer metastasis, inflammatory and autoimmune diseases. To date, around 50 chemokines have been identified in humans. Chemokines can be classified by structure or function. Four families – C, CC, CXC, and CX3C - are distinguished based on the arrangement of cysteine residues involved in the formation of disulfide bonds, and three groups based on their function: proinflammatory, homeostatic, and mixed [47, 48]. Most chemokines are present in soluble form mediating chemotaxis. CX3CL1 and CXCL16 are unique, because they can exist both membrane-bound and soluble form, thus besides chemotaxis they mediate cell-cell adhesion [46, 49]. Chemokine families and their receptors are shown in Fig. 5.

CCL2 (MCP1) is the first discovered and most extensively studied CC chemokine; it is one of the key chemokines that regulate migration and infiltration of monocytes and macrophages. CCL2 is expressed among others by adipocytes and its circulating level correlate with adiposity [50, 51]. Besides CCL2, several other chemokines are also associated with obesity, adipose tissue macrophage infiltration, or adipose tissue inflammation. These are: CCL3, CCL5, CCL7, CCL8, CCL11, CCL19, CXCL1, CXCL5, CXCL8, CXCL10 and CX3CL1 [52-56].



Nature Reviews | Neuroscience

Figure 5. Chemokine families and their receptors. Chemokines are divided into four families based on the number and spacing of the conserved cysteine residues in their amino termini. In CXC (alpha) chemokines (a), one amino acid separates the first two cysteine residues. In CC (beta) chemokines (b), the first two cysteine residues are adjacent to each other. The C (gamma) chemokine subfamily (c) is distinguished structurally as containing only two of the four conserved cysteine residues that are found in the other families. The CX3C (delta) chemokine subfamily, which is currently represented by a single member named fractalkine (CX3CL1), is characterized by the presence of three amino acids between the first two cysteine residues, as well as a transmembrane and mucin-like domain (d).[57].

Chemokine receptors can be divided into two groups: G protein-coupled chemokine receptors, which signal by activating Gi-type G proteins, and atypical chemokine receptors, which appear to shape chemokine gradients and dampen inflammation by scavenging chemokines in an arrestin-dependent manner. Chemokine receptors are differentially expressed by leukocytes and many nonhematopoietic cells [46].

Fractalkine (CX3CL1/neurotactin), the only member of CX3C family, was first described in 1997 [58, 59]. Mature membrane bound fractalkine is a 371 (mouse) or 373 (human) amino acid peptide with four domains: chemokine domain, mucin stalk, transmembrane domain and cytoplasmic domain [59-61]. The structure of fractalkine is shown in Fig. 6A.

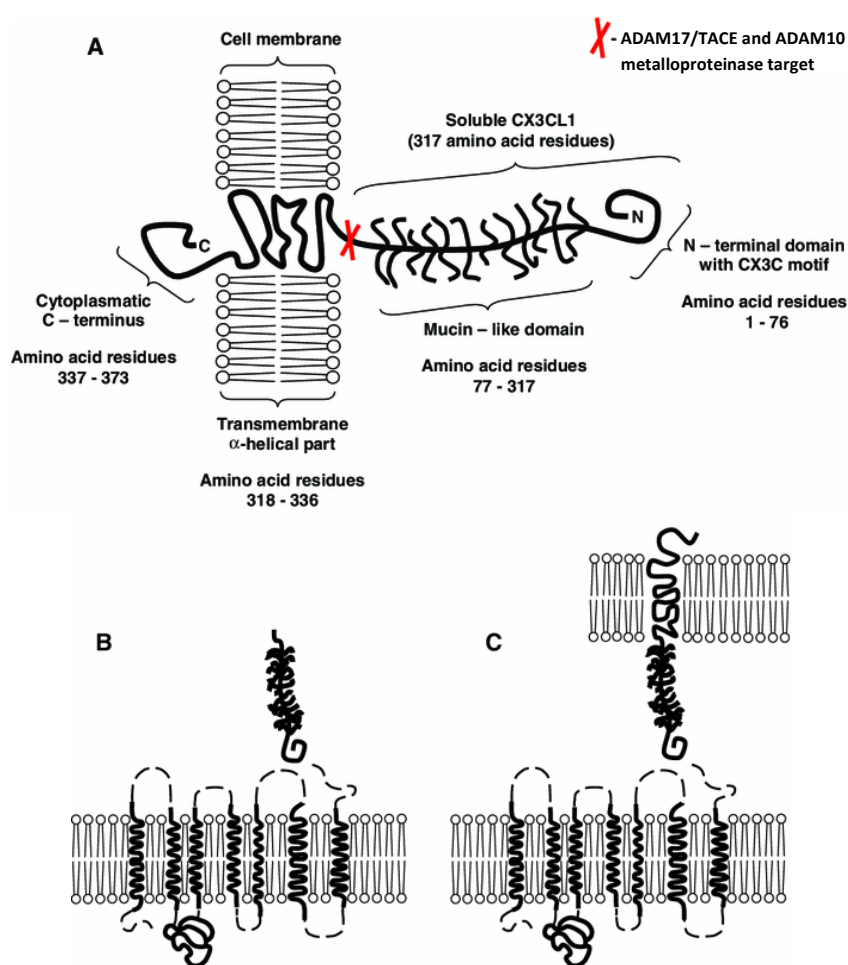


Figure 6. The molecular structure of fractalkine and CX3CR1 and their interaction.

A) The structure of the membrane-bound form of fractalkine showing specific regions of the molecule and the site of the cleaving action of the metalloproteinases ADAM17/TACE and ADAM10. The unbound form of fractalkine (B), produced by metalloproteinase cleaving and the membrane-bound form (C) interacting with the CX3CR1 [62].

Cleavage of fractalkine can be homeostatic or induced (with PMA, m β CD, SLO, or ionomycin), mediated by ADAM10 (the majority of constitutive, and ionomycin-induced shedding) and ADAM17 metalloproteinases [63] resulting a soluble molecule. ADAM17 (TACE) is also responsible for the regulation of the proteolytic release of other chemokines, cytokines, growth factors and their receptors, including TNF α , TNF receptors I and II, TGF α , I-selectin, IL6, and M-CSF receptor 1. Fractalkine shedding by ADAM17 is increased in a variety of diseases such as diabetes, atherosclerosis, ischemia, heart failure, arthritis, cancer, neurological and immune diseases [64]. Elevated mRNA expression of *Adam17* was found in epididymal fat [65], and in subcutaneous fat [66] of HFD fed obese mice. These results suggest that fractalkine shedding is correlated with TNF α release in various diseases.

Fractalkine is expressed in numerous organs, such as brain, lung, kidney, intestines, pancreas, adipose tissue, liver in homeostatic state and it is upregulated in inflammatory conditions. Neurons, epithelial cells, endothelial cells, smooth muscle cells, adipocytes have shown to express fractalkine [56, 59, 67-71].

Analysis of CX3CR1 expression in CX3CR1+/gfp mice showed GFP/CX3CR1 positivity in the following cells: peripheral blood monocytes (CD11b⁺ and Gr1^{low}), a subset of natural killer (NK) cells (5 to 30% of all NK cells), subsets of both CD8 α ⁻ (so-called myeloid) and CD8 α ⁺ (lymphoid) dendritic cells (DCs), macrophages. Within the brain, microglia (the brain resident macrophage population) express fractalkine receptor [67, 72, 73]. CX3CR1 - belongs to the class of metabotropic receptors, also known as G protein-coupled receptors, or seven-transmembrane proteins. [74]. The receptor is coupled to Gi and Gz subtypes of G proteins [75]. The structure of CX3CR1 and its interaction with fractalkine is shown in Fig. 6B-C. CX3CR1 activation by fractalkine have been shown to induce multiple signal transduction pathways leading to elevation of cytosolic free calcium and modifications in enzymes, ion channels, transcriptional activators, and transcriptional regulators [76-80]. Fractalkine signaling eventually participates in the adhesion, chemotaxis and survival of the cells expressing CX3CR1 [80]. Fig. 7. shows the model of fractalkine dependent migration of leukocytes.

Fractalkine is an important regulatory factor of microglia activity in the central nervous system where it mediates neuroinflammation. However, its role in metabolic inflammation in general, and in connecting metabolic and neuroinflammation in particular, remains to be elucidated. It has recently been shown that fractalkine is an adipocytokine in humans [56]. Furthermore, elevated plasma fractalkine levels were detected in patients with type 2 diabetes and single nucleotide polymorphism (rs3732378) in *CX3CR1* was associated with changes in adipose markers and metabolic parameters [56].

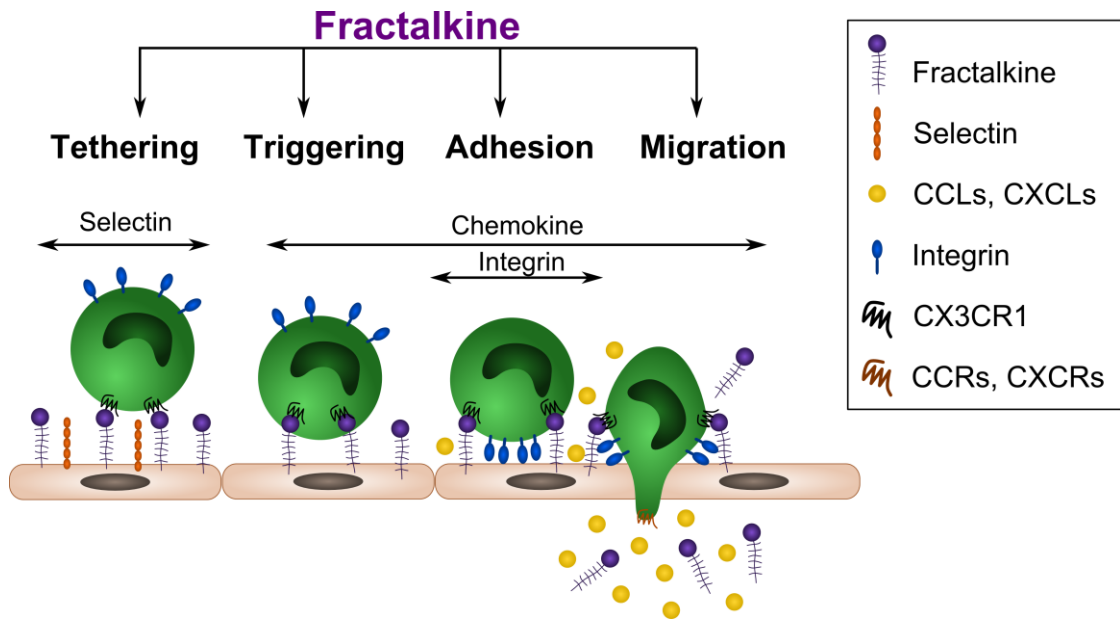


Figure 7. Schematic model of fractalkine-mediated pathways in the adhesion cascade.

Fractalkine is expressed on endothelial cells as the membrane-bound form and captures CX3CR1 expressing leukocytes in a selectin- and integrin-independent manner. Interaction between fractalkine and CX3CR1 can also increase integrin avidity, resulting in firmer adhesion. CX3CR1 expressing leukocytes then extravasate through the vascular wall into the tissue to a chemokine gradient. Fractalkine may facilitate extravasation of circulating CX3CR1 expressing leukocytes by mediating cell adhesion through the initial tethering and final transmigration steps [81].

The role of fractalkine – CX3CR1 signaling in cardiovascular diseases (such as atherosclerosis), rheumatoid arthritis, other inflammatory diseases and cancer is well described [80, 82], however its function in obesity is not fully known. Furthermore, it is not known whether fractalkine – CX3CR1 signaling has a role in BAT inflammation and/or function.

3. Aims

My aims were

- (I) to identify the role of fractalkine/CX3CR1 signaling in the recruitment and activation of immune cells in key central (hypothalamus) and peripheral (visceral WAT, BAT and liver) structures in obesity and,
- (II) to reveal the role of obesity-related, fractalkine – CX3CR1 dependent, local inflammation in regulation of triglyceride- and thermo-metabolism in BAT of obese mice.

4. Materials and methods

4.1. Animals and diet

Experiments were performed in male CX3CR1 +/gfp (+/gfp), and CX3CR1 gfp/gfp (gfp/gfp) mice [83]. Animals were obtained from the European Mouse Mutant Archive (EMMA CX3CR1^{tm1^{Litt}} MGI:2670351). In these mice, the *Cx3cr1* gene was replaced by a *Gfp* reporter gene such that heterozygote CX3CR1 +/gfp mice express GFP and retain receptor function in CX3CR1 expressing cells, whereas homozygote CX3CR1 gfp/gfp mice are labeled with GFP and lack functional CX3CR1. Genotype of the animals has been verified by PCR using combination of three different primers as described by Jung et al [83].

The background C57Bl/6J strain has been shown to be genetically vulnerable to diet-induced obesity [84].

Animals were housed in groups of 4-5/cage at the minimal disease (MD) level of the Medical Gene Technology Unit of our Institute, had free access to food and water and were maintained under controlled conditions: temperature, 21 °C ± 1 °C; humidity, 65%; light-dark cycle, 12-h light/12-h dark cycle, lights on at 07:00. 5-14 weeks old mice, both CX3CR1 +/gfp (n=25) and CX3CR1 gfp/gfp (n=25) mice were randomly distributed into two groups. The first group, normal diet (ND), received standard chow (VRF1 (P), Special Diets Services (SDS), Witham, Essex, UK.). The second group received fat-enriched diet (FatED), by providing a 2:1 mixture of standard chow and lard (Spar Budget, Budapest, Hungary). The energy content and macronutrient composition of the two diets is given in Table 2. All procedures were conducted in accordance with the guidelines set by the European Communities Council Directive (86/609 EEC) and approved by the Institutional Animal Care and Use Committee of the Institute of Experimental Medicine (permit number: 22.1/3347/003/2007).

Table 2. Energy content and macronutrient composition of diets

	ND - standard chow		FatED - mixed chow	
	g%	kcal%	g%	kcal%
Protein	19,1	22,5	12,7	9,7
Carbohydrate	55,3	65,0	36,9	28,0
Fat	4,8	12,6	36,5	62,3
kcal/g	3,40		5,27	

4.2. Experimental design

Mice were fed with normal diet (ND) or fat enriched diet (FatED) for 10 weeks, body weight and food consumption was measured weekly. In the 10th week, glucose tolerance test (GTT) was performed after overnight fasting. Two days after the GTT, mice were decapitated, trunk blood was collected on EDTA, and the plasma stored at -20°C until assay. Brain, liver, visceral- and subcutaneous white adipose tissue pads and interscapular brown adipose tissue were collected, sampled and stored at -70°C for RT-PCR, or fixed in 4% buffered paraformaldehyde for histology. A separate set of animals underwent cold tolerance test. Body composition was assessed on another set of animals.

4.3. Body composition analysis

Body composition was determined using EchoMRI™ Body Composition Analyzer (EchoMRI, Houston, TX, USA). Mice were scanned weekly. Two scans were performed per animal and the average was used for analysis. Body fat composition was calculated by determining total fat (g) divided by total body weight (g) and expressed as a percentage.

4.4. Glucose tolerance test

Mice were fasted overnight (15 h) and then injected intraperitoneally with 2 mg/g of body weight D-glucose (20% stock solution in saline). Blood glucose was measured from tail vein by DCont Personal Blood Glucose Meter (77 Elektronika Kft. Hungary) at 0 min (just before glucose injection) and at 15-, 30-, 60-, 90- and 120-min intervals after the glucose load.

4.5. Hormone and cytokine measurements

Plasma adrenocorticotrophic hormone (ACTH) and corticosterone (CORT) concentrations were measured by radioimmunoassay (RIA). ACTH RIA was developed in our laboratory [85] using an antibody (#8514) raised against the mid-portion of human ACTH1-39. The test uses 50 μ l of plasma per determination, has a lower limit of sensitivity of 0.1 fmol/ml, and the average intra- and inter-assay coefficients of variation are 4.8% and 7.0% respectively. Plasma corticosterone has been measured by a direct RIA without extraction as described [86]. The intra and interassay %CVs in this assay are 12.3 and 15.3 respectively.

Plasma cytokine levels were measured by ELISA using DuoSet ELISA kits for IL1a, IL1b and IL6 (R&D Systems, Minneapolis, MN, USA) according to the manufacturer's protocol.

4.6. Histology and quantitative analysis

Tissue samples were immersion fixed in 4% w/v paraformaldehyde in 0.1 mol l⁻¹ phosphate buffer, pH 7.4 (PB) for 3 days and stored in 1% w/v paraformaldehyde in 0.1 mol l⁻¹ PB at 4°C then were embedded in paraffin, sectioned and stained with hematoxylin-eosin (H&E). Microscopic slides were digitalized with Panoramic Digital Slide Scanner (3DHISTECH Kft., Hungary). WAT adipocyte cell areas and, lipid droplet number and size of brown adipose cells were counted under 40x magnification in one field of view with ImageJ software (NIH, USA). In WAT samples of FatED groups all adipose cells (60-80), while in ND groups maximum 150 cells were analyzed per field. In BAT 31 cells and 401-823 droplets were analyzed per animal.

4.7. Immunohistochemistry

F4/80 (murine macrophage marker) staining on paraffin-embedded tissue sections was performed by standard immunohistochemical protocol. Slides were deparaffinized and rehydrated then antigen retrieval was performed with proteinase K (10 mg/ml; diluted to 1:25 in 1 M Tris buffer pH=8.0). Endogenous peroxidase was blocked by 0.3% H₂O₂. After washes in KPBS, nonspecific binding was blocked by 2% normal rabbit serum for 1 hour. The sections were incubated in anti-mouse F4/80 antibody made in rat (BMA Biomedicals, 1:50) overnight at 4°C. Following KPBS (0.01M potassium phosphate buffer, 0.154 M NaCl pH 7.4) washes (4 x 5 min), slides were incubated for 1 hour in biotinylated rabbit anti-rat antibody (Vector Laboratories; 1:250). After rinsing in KPBS, avidin biotin amplification was performed with a Vectastain Elite ABC kit (Vector Laboratories) and immunoreactivity was visualized by nickel-enhanced diaminobenzidine (DAB-Ni) substrate. Sections were analyzed with Nikon Eclipse E600 microscope under 20x magnification in 5 fields of view per section.

Fluorescent F4/80 labeling was performed on 1 mm³ BAT blocks fixed in 4% w/v paraformaldehyde in 0.1 M phosphate buffer (pH 7.4), and stored in cryoprotectant solution at -20°C. Tissue blocks were treated with 2% normal rabbit serum then incubated in rat anti-mouse F4/80 antibody (BMA Biomedicals; 1:50) overnight at 4°C. The antigens were then visualized by biotinylated rabbit anti-rat IgG (Vector Laboratories; 1:500) for 100 minutes followed by streptavidin Alexa 594 (Molecular Probes; 1:500) for 100 minutes. Images were taken using a Nikon C2 confocal microscope, at 60x magnification.

4.8. Core body temperature measurement and cold challenge

Rectal temperature was measured with Multithermo thermometer (Seiwa Me Laboratories Inc., Tokyo, Japan). To assess cold tolerance, set of animals (N = 30) from both genotypes were fasted for 5 hours, then placed into new individual cages with minimal bedding and transferred to cold room (4°C). Rectal temperature was measured immediately before and 60, 120, 180 and 240 min after cold exposure.

4.9. Gene expression analysis by quantitative real-time PCR

Total RNA was isolated from tissue samples with QIAGEN RNeasyMiniKit (Qiagen, Valencia, CA, USA) according to the manufacturer's instruction. To eliminate genomic DNA contamination, DNase I (Fermentas) treatment was used. Sample quality control and quantitative analysis were carried out by NanoDrop (Thermo Scientific). cDNA synthesis was performed with the High Capacity cDNA Reverse Transcription Kit (Applied Biosystems, Foster City, CA, USA). The designed primers (Invitrogen) were used in real-time PCR reaction with Power SYBR Green PCR master mix (Applied Biosystems, Foster City, CA, USA) on ABI StepOnePlus instrument. The gene expression was analyzed by ABI StepOne 2.3 program. The amplicon was tested by Melt Curve Analysis. Measurements were normalized to ribosomal protein S18 (*Rps18*) expression [87]. Amplification was not detected in the RT-minus controls.

4.10. Primer design

Primers used for the comparative CT (threshold cycle) experiments were designed by the Primer Express 3.0 program. Primer sequences are shown in Table 3.

Table 3. Mouse specific primer sequences used for rtPCR

Gene	Forward sequence	Reverse sequence
<i>Adrb3</i>	ACCGCTCAACAGGTTTGA	GGGGCAACCAGTCAAGAAGAT
<i>Arg1</i>	GTCTGGCAGTTGGAAGCATCT	GCATCCACCCAAATGACACA
<i>Atgl</i>	GCCATGATGGTGCCCTATACT	TCTTGGCCCTCATCACCAGAT
<i>Ccl2 (Mcp1)</i>	CCAGCACCAGCACCAGCCAA	TGGATGCTCCAGCCGGCAAC
<i>Crh</i>	CGCAGCCCTTGAATTCTTG	CCCAGGCGGAGGAAGTATTCTT
<i>Cx3cl1</i>	CCGCGTTCTTCCATTTGTGT	GGTCATCTTGTGCGACATGATT
<i>Dgat1</i>	GTTCCGTCCAGGGTGGTAGT	CGCACCTCGTCTCTTCTAC
<i>Dio2</i>	ACAAACAGGTTAAACTGGGTGAAG	CGTGCACCACACTGGAATTG
<i>Gapdh</i>	TGACGTGCCGCCTGGAGAAA	AGTGTAGCCCAAGATGCCCTTCAG
<i>Gfp</i>	GGACGACGGCAACTACAAGA	AAGTCGATGCCCTTCAGCTC
<i>Glut4</i>	AGGAACTGGAGGGTGTGCAA	GGATGAAGTGCAAAGGGTGAG
<i>Gpat</i>	AGTGAGGACTGGGTTGACTG	GCCTCTCCGGCTCATAAGG
<i>Hsd11b1</i>	CCTCCATGGCTGGGAAAAT	AAAGAACCCATCCAGAGCAAAC
<i>Hsl</i>	AGCCTCATGGACCCTCTTCTA	TCTGCCTCTGTCCCTGAATAG
<i>Il10</i>	AGTGAGAAGCTGAAGACCCTCAGG	TTCATGGCCTTG TAGACACCTTGGT
<i>Il1a</i>	CCATAACCCATGATCTGGAAGAG	GCTTCATCAGTTTGTATCTCAAATCAC
<i>Il1b</i>	CTCGTGGTGTCCGACCCATATGA	TGAGGCCCAAGGCCACAGGT
<i>Il6</i>	CTCTGCAAGAGACTTCCATCC	AGTCTCCTCTCCGGACTTGT
<i>Mgat</i>	TGGTCTGTTTCCCGTTGTTT	GAAACCGGCCCGTTACTCAT
<i>Mgl</i>	CTTGCTGCCAAACTGCTCAA	GGTCAACCTCCGACTTGTTC
<i>Nlrp3</i>	CAGAGCCTACAGTTGGGTGAA	ACGCCTACCAGGAAATCTCG
<i>Npy</i>	CAGATACTACTCCGCTCTGCGACACTACAT	TTCCTTCATTAAGAGGTCTGAAATCAGTGT
<i>Pgc1a</i>	ATGTGCAGCCAAGACTCTGT	TTCCGATTGGTCGCTACACC
<i>Pomc</i>	TGCTTCAGACCTCCATAGATGTGT	GGATGCAAGCCAGCAGGTT
<i>Pparg2</i>	CTCCTGTTGACCCAGAGCAT	TGGTAATTTCTTGTGAAGTGCTCA
<i>Rps18</i>	TCCAGCACATTTTGCAGTA	TTGGTGAGGTCGATGTCTGC
<i>Th</i>	TCTCAGAGCAGGATACCAAGCA	GCATCCTCGATGAGACTCTGC
<i>Tnfa</i>	CAGCCGATGGGTTGTACCTT	GGCAGCCTTGTGCCTTGA
<i>Ucp1</i>	GGTCAAGATCTTCTCAGCCG	AGGCAGACCGCTGTACAGTT

4.11. Normalized *Gfp* expression

Because the coding region of the *Cx3cr1* gene has been replaced by *Gfp* in experimental animals [83], I relied on *Gfp* expression to estimate and compare *Cx3cr1* gene expression in CX3CR1 homo-(*gfp/gfp*) and heterozygote (+/*gfp*) animals. To resolve different *Gfp* copy numbers in homo- and heterozygotes, normalized *Gfp* expression was calculated using the following formula: RQ / CN , where RQ is the relative quantity of *Gfp* from real time qPCR measurement and CN is the *Gfp* copy number determined from genomic DNA by Taqman Copy Number Assay.

4.12. Western blot analysis

BAT samples were homogenized by Bertin Minilys homogenizer in RIPA buffer (50mM Tris - 150mM NaCl - 1% Triton X-100 - 0,5% Na deoxycholate - 0,1% SDS pH=8.0) supplemented with protease inhibitor cocktail tablet (Compleat Mini per 10 ml, Roche). Protein samples (20 μ g) were separated by electrophoresis on 12% SDS gel at 120 V for 2 h and transferred to Hybond-ECL membrane (Amersham Life Science) by semi-dry transfer (Trans Blot SD Cell, Biorad). The transfer was carried out at 24 V for 60 min using ice cold transfer buffer (20mM Tris - 190mM Glycine - 20% Methanol pH=8.3). The membrane was incubated for 1 h in blocking buffer (1xTBST:154mM Trizma base - 1,37M NaCl - 0.05% Tween-20 pH=7.6 and 5% non-fat dry milk). After incubation, the membrane was cut between 49kDA and 37kDA marks (Benchmark pre-stained protein ladder, Invitrogene). Thereafter, membranes were probed either by rabbit anti-UCP1 antibody (1:1000, Abcam) or mouse monoclonal anti- β -tubulin antibody (1:2000; Proteintech). Both membranes were washed three times for 5 min in $1 \times$ TBST before 1h incubation in buffer ($1 \times$ TBS, 0.05% Tween-20) containing biotinylated anti-rabbit IgG (1:5000, Vector) or HRP conjugated anti-mouse IgG (1:4000, Sigma) respectively. Membrane, containing UCP1, was incubated 1h in avidin-biotin horseradish peroxidase complex (Vectastain Elite ABC Peroxidase Kit, Vector). Afterwards both membranes were developed by immunoperoxidase reaction. Images were acquired by Chemi Genius 2 Bioimaging System (Syngene) and analyzed using ImageJ software. UCP1 values were normalized to those for tubulin.

4.13. Stromal Vascular Fraction preparation and Flow Cytometry

Epididymal white fat pads have been dissected from mice after decapitation. Fat tissue was minced into small pieces and digested in Krebs-Ringer HEPES (KRH) buffer (pH=7.4) containing 1% BSA and 1mg/ml Collagenase (SIGMA C9891) at 37°C for 30 min in shaking bath and then filtered through a 40 µm mesh. The cell suspension was centrifuged at 500x g for 10 min. to separate floating adipocytes and stromal vascular cell fraction (SVF) in the pellet. SVF was resuspended in KRH-BSA buffer. Following lysis of red blood cells with ACK solution and Fc receptor blockade (anti-mouse CD16/CD32, clone 93, eBioscience), cells were labelled with cocktails of selected antibodies: MHCII-APC, Ly6c-PE-Cy7, CD115-APC (eBioscience) and F4/80-PE (Serotec). Specificity of antibodies has been assessed by eBioscience and Serotec, respectively. Cells were acquired on a FACSAria II flow cytometer (BD Biosciences, US) and data were analyzed using FACS Diva software (BD Biosciences).

4.14. Statistical analysis

Statistical analysis was performed by factorial ANOVA with Newman–Keuls post-hoc test in Statistica 11 (StatSoft Inc.). Flow cytometric data were analyzed by two-way ANOVA followed by Sidak’s multiple comparison test (GraphPad Prism). The results are shown as means ± SEM. Main effects of ANOVA are presented in the text, the post-hoc results are shown in the graphs. If the main effect was significant, but the post-hoc did not show differences, the main effects are shown in the graph. In all cases $p < 0.05$ was considered significant.

5. Results

5.1. Fractalkine – CX3CR1 signaling is necessary for the development of the characteristics of obesity

5.1.1. Body weight gain, body fat gain

To investigate the role of fractalkine – CX3CR1 signaling in the development of obesity, mice with intact (CX3CR1 +/gfp) or impaired (CX3CR1 gfp/gfp) fractalkine signaling were fed with ND or FatED for 10 weeks. Body weight gain, food and energy intake and, fecal output was monitored regularly.

Body weight gain became significant from the 5th week in response to FatED. Although the body weight elevated in both genotypes, it was statistically significant only in +/gfp FatED mice (Fig. 8A). (Factorial ANOVA: W5 diet effect: $F(1,46) = 10.40$, $p < 0.01$; W6 diet effect: $F(1,46) = 11.73$, $p < 0.01$; W7 diet effect: $F(1,46) = 15.85$, $p < 0.001$; diet*genotype: $F(1,46) = 4.28$, $p < 0.05$; W8 diet effect: $F(1,46) = 18.53$, $p < 0.001$; genotype effect: $F(1,46) = 4.86$, $p < 0.05$; diet*genotype: $F(1,46) = 4.29$, $p < 0.05$; W9 diet effect: $F(1,46) = 23.37$, $p < 0.001$; genotype effect: $F(1,46) = 4.99$, $p < 0.05$; diet*genotype: $F(1,46) = 4.67$, $p < 0.05$; W10 diet effect: $F(1,46) = 26.38$, $p < 0.001$; diet*genotype: $F(1,46) = 6.03$, $p < 0.05$)

The increased body weight gain might be the result of elevated energy intake, elevated energy harvest from food or decreased energy expenditure. I did not find differences in food and energy intake or feces amount between genotypes (Table 4-6).

Although the daily food consumption and feces amount of all FatED mice was lower, the daily energy intake was comparable to those that are on normal diet. Because there were no significant genotype effect in above mentioned parameters, these factors may not be responsible for the differences seen in body weight gain.

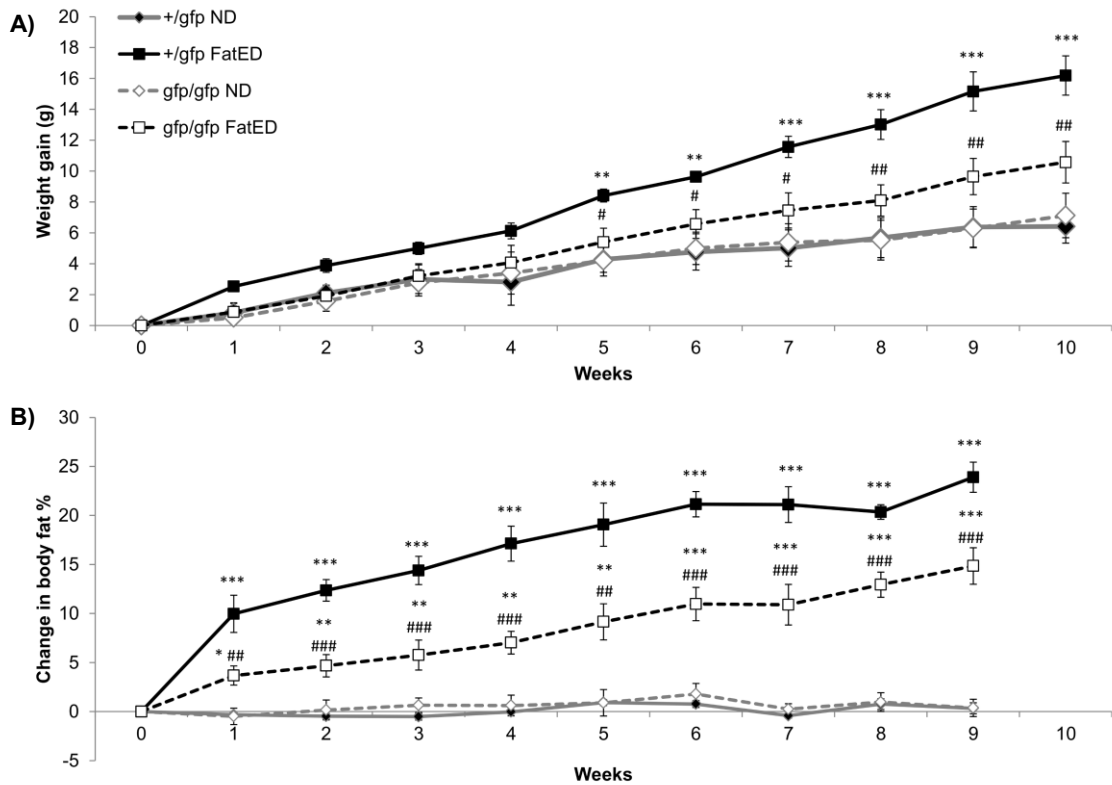


Figure 8. Fractalkine signaling contributes to weight gain in FatED fed mice.

A) Weight gain in control (*CX3CR1* +/gfp) and fractalkine receptor deficient (*CX3CR1* gfp/gfp) mice during 10 weeks of ND or FatED. $N = 12-13$ per group. B) Change in body fat% measured by EchoMRI. $N = 3-4$ per group. Mean \pm SEM values, * $p < 0.05$; ** $p < 0.01$; *** $p < 0.001$ vs. ND, # $p < 0.05$; ## $p < 0.01$; ### $p < 0.001$ vs. +/gfp (Newman-Keuls post-hoc comparison). FatED – fat enriched diet, ND – normal diet.

EchoMRI showed that body weight gain in FatED fed mice was the result of body fat gain (Fig. 8B).

5.1.2. Fat depots

By analyzing fat depots I found that the relative weight of EWAT – which is responsible for fat storage – and BAT – which participates in energy expenditure by thermogenesis – was increased in response to FatED, but it was significantly lower in gfp/gfp mice (Fig. 9A-B) (EWAT: diet effect: $F(1,28) = 34.90$, $p < 0.001$; genotype effect: $F(1,28) = 5.75$, $p < 0.05$; diet*genotype: $F(1,28) = 4.30$, $p < 0.05$; BAT: (diet effect: $F(1,28) = 27.52$, $p < 0.001$). Relative liver weight was lower in FatED fed mice, but there were no differences between genotypes (Fig.9C) (diet effect: $F(1,14) = 71.10$, $p < 0.001$).

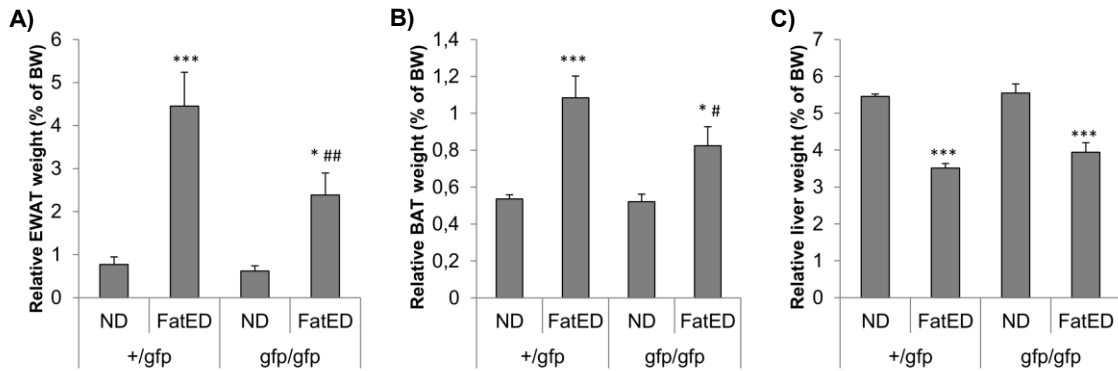


Figure 9. Adipose tissue and liver weights are affected by fractalkine signaling in *FatED* fed mice. Normalized organ weights are shown as % of body weight. A) EWAT, $N = 7-9$ per group. B) BAT, $N = 8-9$ per group. C) Liver, $N = 4-5$ per group. Mean \pm SEM values, * $p < 0.05$; ** $p < 0.01$; *** $p < 0.001$ vs. ND, # $p < 0.05$; ## $p < 0.01$; ### $p < 0.001$ vs. +/gfp (Newman-Keuls post-hoc comparison). FatED – fat enriched diet, ND – normal diet.

Table 4. Daily food intake (g) / mouse.

Genotype	Diet	Weeks									
		1	2	3	4	5	6	7	8	9	10
+/gfp	ND	3,41 \pm 0,58	4,63 \pm 0,28	3,97 \pm 0,37	4,52 \pm 0,14	4,45 \pm 0,15	3,69 \pm 0,15	7,33 \pm 0,37	3,99 \pm 0,34	4,9 \pm 0,26	3,31 \pm 0,36
	FatED	2,88 \pm 0,11	3,38 \pm 0,11*	2,58 \pm 0,1**	2,83 \pm 0,08***	2,84 \pm 0,18***	3,24 \pm 0,16	3,17 \pm 0,15	3,03 \pm 0,1	3,02 \pm 0,16	3,53 \pm 0,24
gfp/gfp	ND	3,53 \pm 0,53	5,75 \pm 0,79#	4,14 \pm 0,15	4,69 \pm 0,36	4,44 \pm 0,27	4,23 \pm 0,35	6,62 \pm 0,11	4,38 \pm 0,8	5,15 \pm 0,16	4,1 \pm 0,26
	FatED	2,7 \pm 0,09	3,25 \pm 0,19**	2,68 \pm 0,19**	2,88 \pm 0,22***	2,74 \pm 0,08***	3,32 \pm 0,23*	3,07 \pm 0,19	2,9 \pm 0,13*	2,94 \pm 0,16	3,37 \pm 0,14

Mean \pm SEM values. * $p < 0.05$; ** $p < 0.01$; *** $p < 0.001$ vs. ND; # $p < 0.05$ vs. +/gfp (Newman-Keuls post-hoc comparison). $N = 4-5$ per group.

Table 5. Daily energy intake (kcal) / mouse.

Genotype	Diet	Weeks									
		1	2	3	4	5	6	7	8	9	10
+/gfp	ND	11,59 ± 1,99	15,74 ± 0,96	13,5 ± 1,26	15,4 ± 0,5	15,13 ± 0,53	12,55 ± 0,51	24,93 ± 1,26	13,59 ± 1,15	16,66 ± 0,89	11,27 ± 1,25
	FatED	15,14 ± 0,6	17,82 ± 0,62	13,6 ± 0,53	14,92 ± 0,46	14,95 ± 0,98	17,07 ± 0,85	16,69 ± 0,83***	15,95 ± 0,53	15,92 ± 0,86	18,56 ± 1,27**
gfp/gfp	ND	12,01 ± 1,82	19,56 ± 2,68	14,08 ± 0,53	15,95 ± 1,23	15,09 ± 0,94	14,38 ± 1,22	22,5 ± 0,37	14,91 ± 2,74	17,52 ± 0,55	13,94 ± 0,89
	FatED	14,2 ± 0,52	17,13 ± 1	14,09 ± 1,05	15,14 ± 1,16	14,45 ± 0,43	17,5 ± 1,21	16,17 ± 1,03**	15,28 ± 0,7	15,5 ± 0,88	17,73 ± 0,77 *

Mean ± SEM values, ** p < 0.01; *** p < 0.001 vs. ND (Newman-Keuls post-hoc comparison). N = 4-5 per group.

Table 6. Daily fecal output (g) / mouse.

Genotype	Diet	Weeks					
		1	3	4	6	7	8
+/gfp	ND	0,93 ± 0,04	0,93 ± 0,04	0,85 ± 0,04		0,89 ± 0,02	0,99 ± 0,07
	FatED	0,52 ± 0,04***	0,54 ± 0,02***	0,47 ± 0,03***	0,51 ± 0,03	0,42 ± 0,01***	0,44 ± 0,02***
gfp/gfp	ND	0,95 ± 0,03	0,91 ± 0,08	0,81 ± 0,03		0,96 ± 0,16####	1,02 ± 0,03
	FatED	0,51 ± 0,01***	0,55 ± 0,02***	0,49 ± 0,02***	0,51 ± 0,02	0,43 ± 0,01***	0,48 ± 0,01***

Mean ± SEM values, *** p < 0.001 vs. ND, #### p < 0.001 vs. +/gfp (Newman-Keuls post-hoc comparison). N = 4-5 per group.

5.1.3. Glucose intolerance

Obesity is often associated with glucose intolerance, which was observed following GTT in +/gfp FatED mice but not in gfp/gfp FatED group. During the first 60 minutes after glucose load, there were no differences between groups. However after 120 minutes, blood glucose levels returned to normal in ND groups and gfp/gfp FatED fed mice, but not in +/gfp FatED group (diet effect: F (1,14) = 8.51, p < 0.05; diet*genotype: F (1,14) = 5.10, p < 0.05) (Fig.

10B). Fasting blood glucose levels were similar in all groups, which means that 10 weeks of FatED did not cause severe dysregulation in carbohydrate metabolism (Fig. 10A).

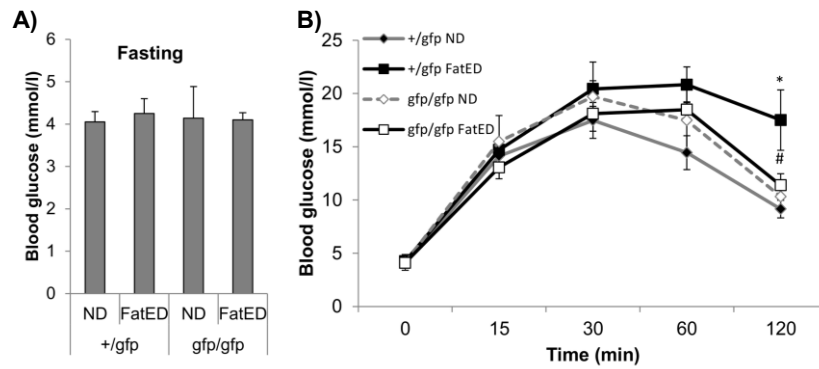


Figure 10. Effects of fat enriched diet on glucose homeostasis

A) Fasting blood glucose levels ($N = 4-5$ per group). B) Blood glucose levels in response to ip. glucose load during glucose tolerance test. *CX3CR1* *gfp/gfp* mice kept on fat-enriched diet did not develop glucose intolerance ($N = 4-5$ per group). * $p < 0.05$ vs. ND, # $p < 0.05$, ## $p < 0.01$ vs. +/gfp (Newman-Keuls post-hoc comparison). FatED – fat enriched diet, ND – normal diet.

5.1.4. Cold tolerance

Cold tolerance test was performed to examine the thermogenic ability of mice. The core temperature at the beginning of the test was not statistically different between groups (Fig. 11A), although it seems to be lower in FatED groups. When mice were placed to cold, the rectal temperature of all mice gradually decreased. However, after 2 hours in cold, the temperature of homozygous animals started to increase back to the normal and the increase in FatED mice was significantly higher than that seen in heterozygous animals fed by control- or FatED (genotype effect: $F(1,26) = 4.75$, $p < 0.05$). It should be noted that the decrease in body temperature in +/gfp mice seems to be lower in FatED group than in ND group, but it is not statistically significant (Fig. 11B-C).

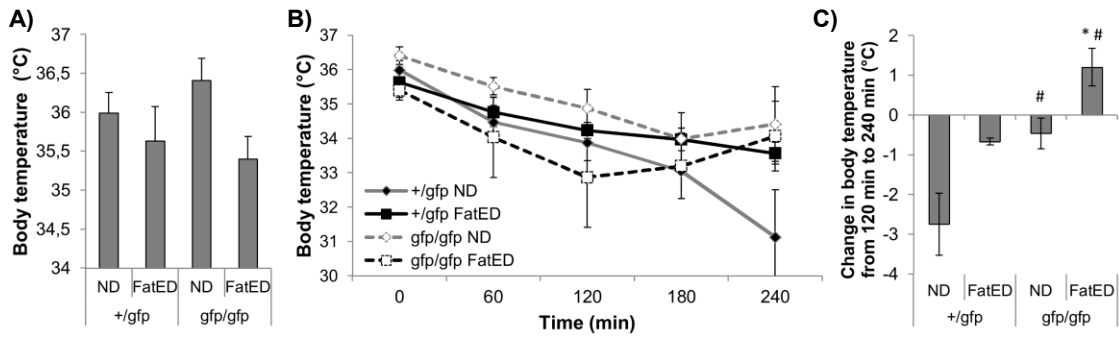


Figure 11. Body temperatures in various temperatures. A) Core body temperature at room temperature. B-C) Changes in body temperature during cold tolerance test. ($N = 13$ in ND groups and $N = 3$ in FatED groups). * $p < 0.05$ vs. ND, # $p < 0.05$ vs. +/gfp (Newman–Keuls post hoc comparison). FatED – fat enriched diet, ND – normal diet.

5.1.5. Elevated plasma cytokine concentrations

Plasma IL1b showed an increase in response to FatED overall (genotype effect: $F(1, 12) = 17.35$, $p < 0.05$). However, post hoc comparison revealed that only +/gfp mice fed a fat-enriched diet showed significant increase in plasma IL1b compared to normal diet, but not gfp/gfp animals. Plasma IL1a and IL6 levels were not significantly different in any experimental groups (Figure 12).

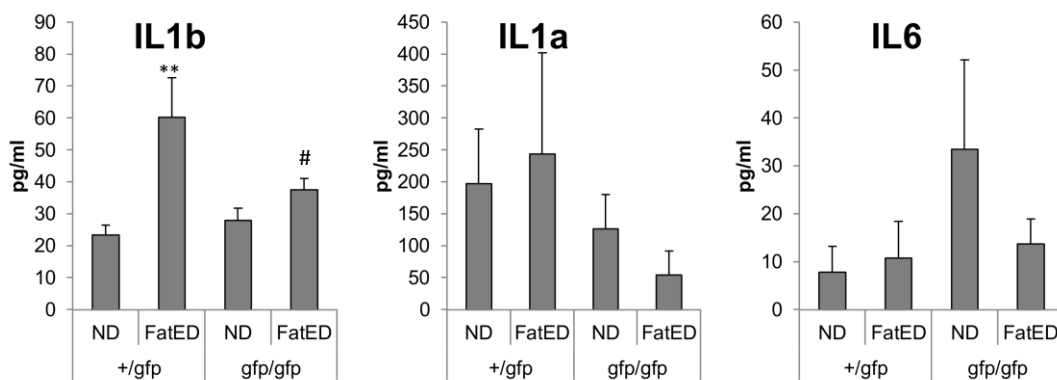


Figure 12. Plasma IL1b is upregulated in response to fat enriched diet in +/gfp, but not in gfp/gfp mice

IL1b, IL1a and IL6 levels were measured from plasma samples with ELISA after 10 weeks of FatED or ND. $N = 4-5$ per group. ** $p < 0.01$ vs. ND, # $p < 0.05$ vs. +/gfp (Newman–Keuls post hoc comparison). FatED – fat enriched diet, ND – normal diet.

5.1.6. Hypothalamo-pituitary-adrenocortical (HPA) axis

Because the neuroendocrine stress axis has been implicated in central metabolic and immune regulation, I assessed corticotropin-releasing hormone (*Crh*) mRNA levels in the hypothalamus and adrenocorticotropin (ACTH) and corticosterone concentration in the plasma. In the hypothalamus there were no significant differences in *Crh* mRNA levels, although a trend towards CX3CR1 *gfp/gfp* mice having slightly elevated *Crh* levels was seen (not significant, (F (1,14) = 3.15, $p = 0.09$) (Fig. 13A)).

Plasma ACTH levels were higher in FatED fed mice than in controls (F (1,13) = 7.35, $p < 0.05$) (Fig. 13B).

Gfp/gfp mice had higher plasma corticosterone levels compared to heterozygotes (+/*gfp*) (F (1,12) = 5.30, $p < 0.05$) (Fig. 13C). The diet was without any significant effect on plasma corticosterone levels.

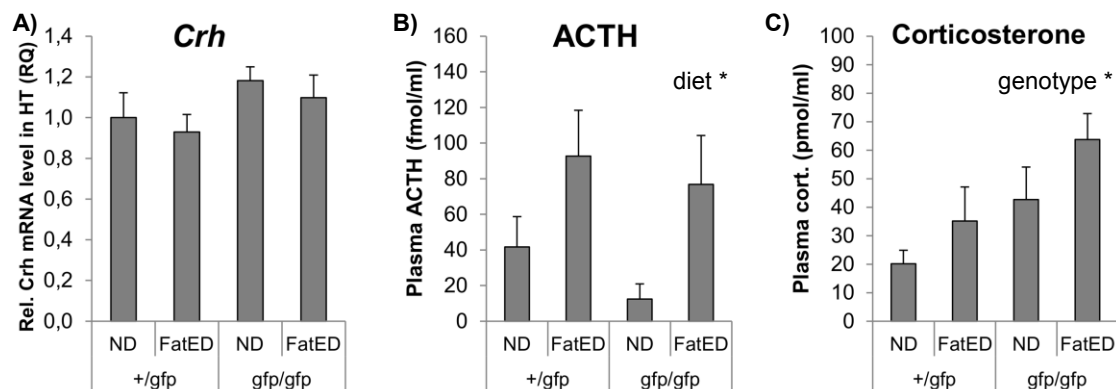


Figure 13. Effect of fat-enriched diet on the activity of the hypothalamo-pituitary-adrenocortical axis

A) Mean ± SEM values of relative *Crh* mRNA levels in the hypothalamus. B) Plasma ACTH-levels * $p < 0.05$ between ND and FatED groups (diet effect). C) Plasma corticosterone levels * $p < 0.05$ between *gfp/gfp* and +/*gfp* groups (genotype effect). $N = 4-5$ per group. FatED – fat enriched diet, ND – normal diet.

5.2. Fractalkine – CX3CR1 signaling dependent adipose tissue remodeling

Histological analysis showed that adipocytes in EWAT and SWAT were enlarged in both FatED groups, but their size was smaller in *gfp/gfp* mice (Fig. 14) (EWAT: diet effect $F(1,1716) = 1403.58$, $p < 0.001$; genotype effect $F(1,1716) = 104.38$, $p < 0.001$; diet*genotype $F(1,1716) = 116.00$, $p < 0.001$; SWAT: diet effect $F(1,2546) = 1099.63$, $p < 0.001$; genotype effect $F(1,2546) = 43.60$, $p < 0.001$; diet*genotype $F(1,2546) = 36.00$, $p < 0.001$).

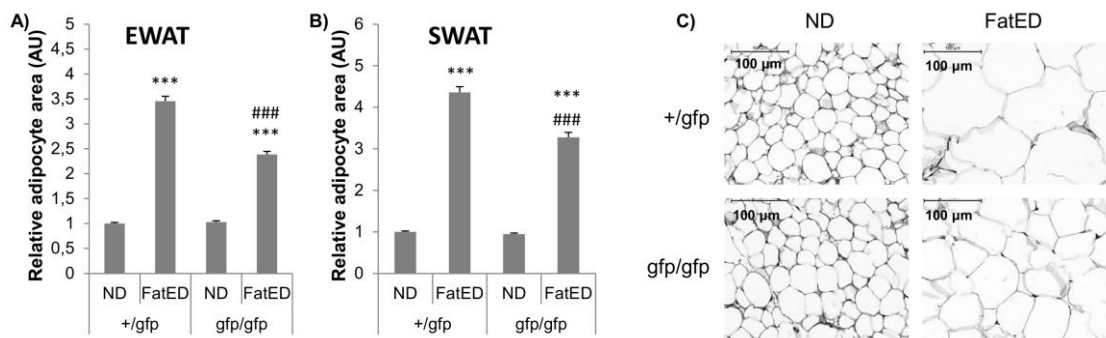


Figure 14. Effect of fat-enriched diet on different fat depots

A-B) Mean \pm SEM values of adipocyte areas measured in EWAT and SWAT samples of *CX3CR1* *gfp/gfp*, and *+gfp* animals kept on normal or FatED ($N = 4-5$ per group). (C) Representative histological images of hematoxylin-eosin stained EWAT sections. Scale bar = 100 μm . *** $p < 0.001$ vs. ND, ### $p < 0.001$ vs. *+gfp* (Newman-Keuls post-hoc comparison). FatED – fat enriched diet, ND – normal diet.

As shown in Fig. 15A, fat enriched diet resulted in “whitening” of BAT. Enlarged brown adipocytes with few large lipid droplets were found in *+gfp* FatED mice, reminiscent of white adipocytes filled with a single lipid droplet were also present. In *gfp/gfp* mice kept on FatED, multilocular brown adipocytes were more abundant than in *+gfp* FatED mice and comparable to BAT cells in ND mice. Due to the coalescence of lipid droplets, the number of lipid droplets per brown adipocytes decreased in response to FatED ($F(1,14) = 90.99$, $p < 0.001$) - but the decrease was moderate in *gfp/gfp* FatED mice (Fig. 15B). Frequency distribution analysis of lipid droplet areas in BAT revealed that FatED shifted the droplet areas to larger sizes, less droplets were under 15 μm^2 and more over 135 μm^2 ($F(1,14) = 8.62$, $p < 0.05$; $F(1,14) = 16.76$, $p < 0.01$, respectively). In *gfp/gfp* FatED mice significantly more small lipid droplets were present than in *+gfp* heterozygotes (Fig. 15C).

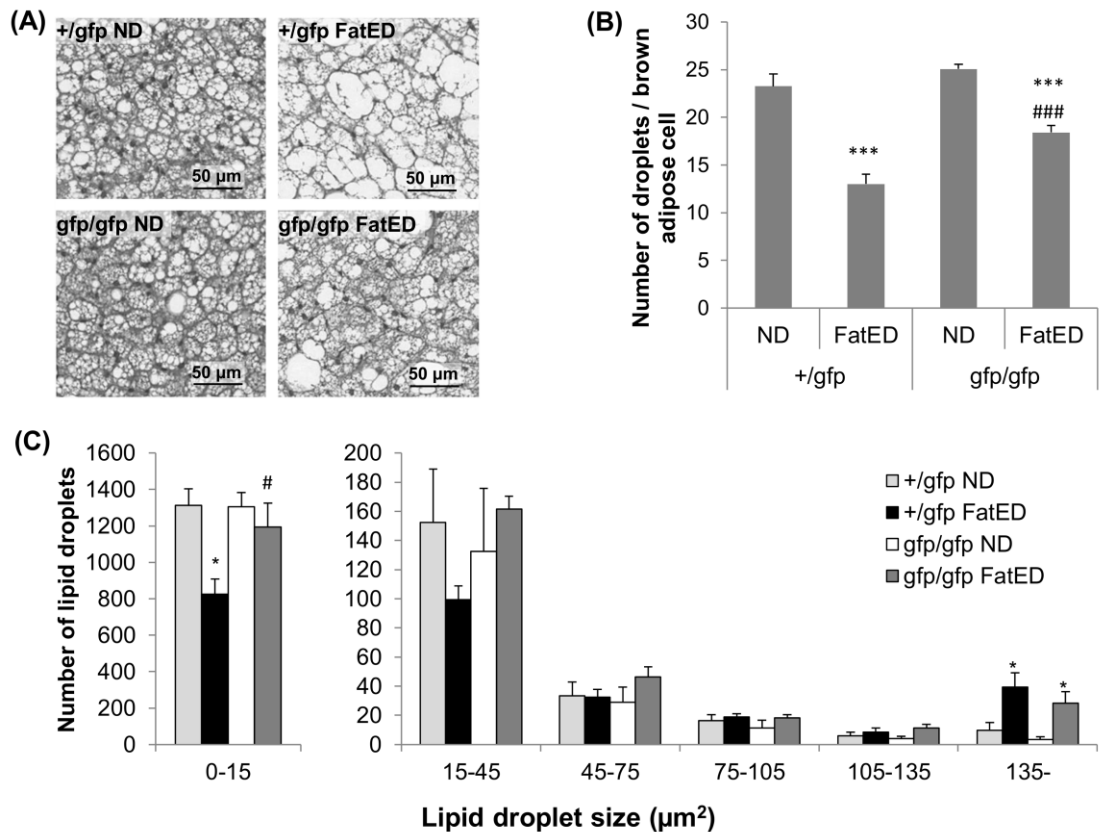


Figure 15. Quantitative histological analysis of BAT

A) Representative histological images of hematoxylin-eosin stained BAT sections. FatED fed *CX3CR1 +gfp* mice have larger lipid droplets. Scale bars = 50 μm . B) Average number of lipid droplets / brown adipose cell. C) Frequency distribution of lipid droplet areas in one field of view. $N = 4-5$ per group. * $p < 0.05$ vs. ND, ** $p < 0.01$ vs. ND, # $p < 0.05$ vs. *+gfp*, ## $p < 0.01$ vs. *+gfp* (Newman-Keuls post hoc comparison). FatED – fat enriched diet, ND – normal diet.

5.3. Accumulation of macrophages to adipose tissues is fractalkine – CX3CR1 signaling dependent

Important feature of obesity is the chronic low grade inflammation and accumulation of macrophages into adipose tissues. Inflammation in obesity starts in adipose tissue, but affects many organs [88].

I confirmed with multiple methods that fractalkine – CX3CR1 signaling plays a role in macrophage accumulation into adipose tissues:

5.3.1. F4/80 Immunohistochemistry

To evaluate the amount of macrophages in the adipose tissues, I performed F4/80 macrophage staining and counted the “crown-like structures” (CLS), because >90% of macrophages infiltrating the adipose tissue of obese animals and humans are arranged around dead adipocytes, forming CLS [89].

The number of CLS was dramatically increased in the EWAT of obese CX3CR1 +/gfp mice, but not in CX3CR1 gfp/gfp mice kept on FatED (diet effect $F(1,16) = 18.37$, $p < 0.001$; genotype effect $F(1,16) = 26.04$, $p < 0.001$; diet*genotype $F(1,16) = 18.37$, $p < 0.001$). Number of CLS in the SWAT of different animals was not significant (Fig. 16).

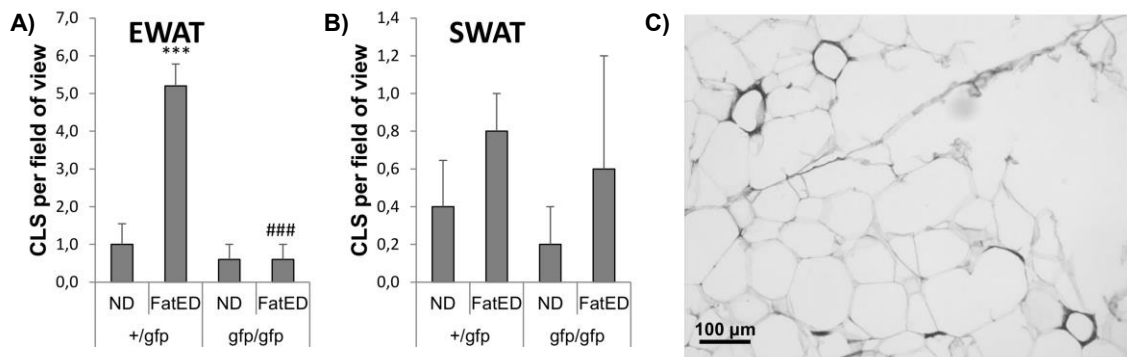


Figure 16. Macrophage accumulation to EWAT and SWAT and formation of CLS.

A) and B) Mean \pm SEM values for CLS per field of view in EWAT and SWAT ($N = 5$ per group). C) Representative image of F4/80 immunostained EWAT of +/gfp FatED mouse. Adipocytes are surrounded by F4/80 positive macrophages and form CLS. Scale bar = 100 μm . B) *** $p < 0.001$ vs. ND, ### $p < 0.001$ vs. +/gfp (Newman–Keuls post hoc comparison). FatED – fat enriched diet, ND – normal diet.

Because little is known about BAT macrophage population, first, fluorescent F4/80 immunostaining was carried out on GFP expressing BAT blocks to make sure that GFP positive cells are similar to those that express the murine macrophage marker F4/80. GFP and F4/80 signals completely colocalized (Fig.17).

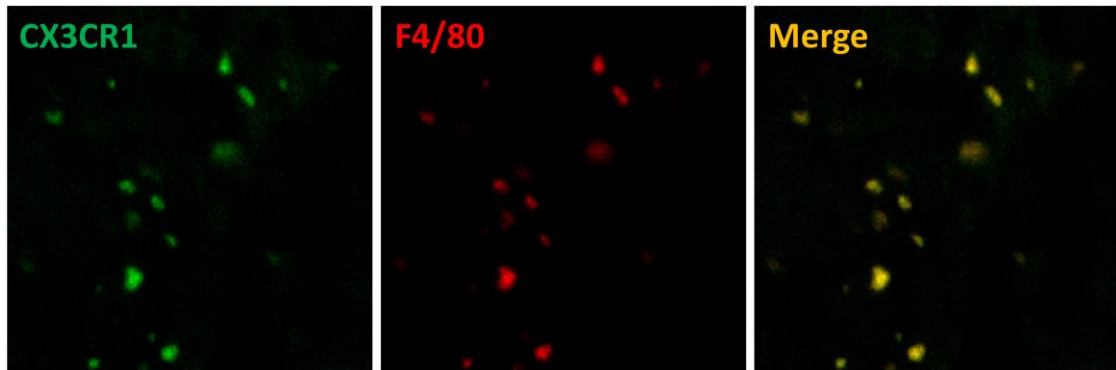


Figure 17. Colocalization of GFP in CX3CR1 expressing cells with F4/80 in the BAT of CX3CR1 +/gfp FatED mouse.

In F4/80 immunostained paraffin embedded BAT sections CLS - similar to those found in WAT of obese animals - were observed: enlarged adipocytes filled with single lipid droplet were surrounded by numerous immune cells in FatED +/gfp mice. Elevated number of CLS was found in BAT in response to FatED ($F(1,14) = 21.46$, $p < 0.001$) but only in +/gfp mice (Fig. 18).

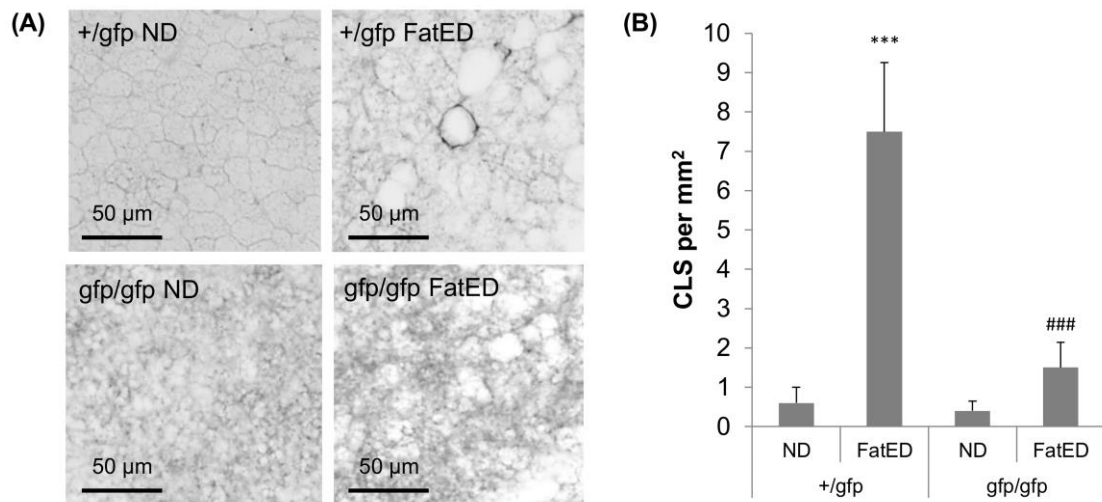


Figure 18. Macrophage accumulation to BAT and formation of CLS

A) Representative images of F4/80 immunostained BAT. Adipocytes with enlarged lipid droplets in the BAT of CX3CR1 +/gfp mice are surrounded by F4/80 positive macrophages and form CLS. Scale bar = 50 μm . B) Mean \pm SEM values for CLS per mm² in BAT ($N = 5$ per group). *** $p < 0.001$ vs. ND, ### $p < 0.001$ vs. +/gfp (Newman-Keuls post hoc comparison). FatED – fat enriched diet, ND – normal diet.

5.3.2. Gfp mRNA expression

To quantify the recruitment of macrophages in the adipose tissues in response to fat-enriched diet, I took advantage of GFP expression in these cells and analyzed normalized *Gfp* mRNA tissue levels. qPCR measurements confirmed the macrophage accumulation both in WAT and BAT. In CX3CR1 +/gfp mice, FatED resulted in an increase of *Gfp* expression, however, in CX3CR1 homozygotes the relative quantity of *Gfp* did not change significantly in response to FatED. In BAT the *Gfp* expression was lower in both diet groups in CX3CR1 gfp/gfp mice than in +/gfp mice, and although it slightly elevated in response to FatED (which was not significant) it was still the half of *Gfp* level measured in +/gfp ND mice. These results suggest that lack of fractalkine receptor impair the infiltration of CX3CR1+ monocytes into adipose tissues (Fig.19). (EWAT: diet effect: $F(1,13) = 11.31$, $p < 0.01$; BAT: diet effect: $F(1,11) = 8.68$, $p < 0.05$; genotype effect: $F(1,11) = 38.97$, $p < 0.001$).

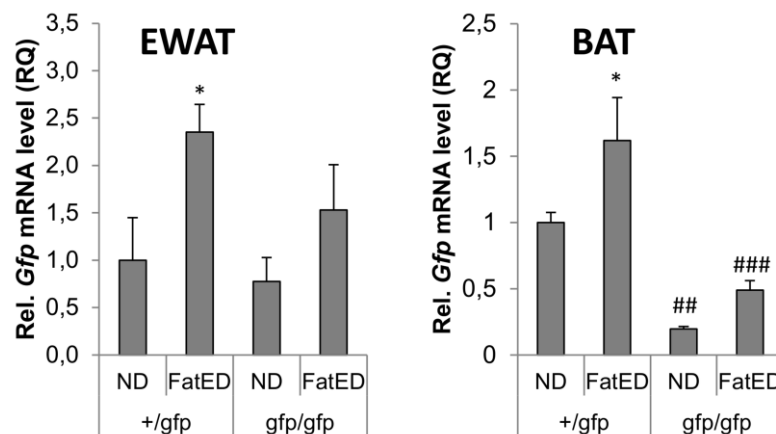


Figure 19. Relative expression of *Gfp* in EWAT and BAT

Mean \pm SEM values for relative mRNA levels in EWAT and BAT. $N = 4-5$ per group. * $p < 0.05$, ## < 0.01 , ### < 0.001 vs. +/gfp (Newman-Keuls post-hoc comparison). FatED – fat enriched diet, ND – normal diet.

5.3.3. FACS analysis

Monocytes and macrophages in the EWAT have been analyzed by flow cytometry. CX3CR1 gfp/gfp mice fed normal chow diet showed significantly reduced macrophage numbers overall (Fig. 20, $p < 0.01$, two-way ANOVA), which was most apparent in the F4/80+ MHCII^{high} population ($p < 0.05$, two way ANOVA followed by Sidak's multiple comparison test)

compared to CX3CR1 +/gfp animals. Numbers of Ly6c^{high} CD115+ or Ly6c^{low} cells were not different between genotypes (not shown).

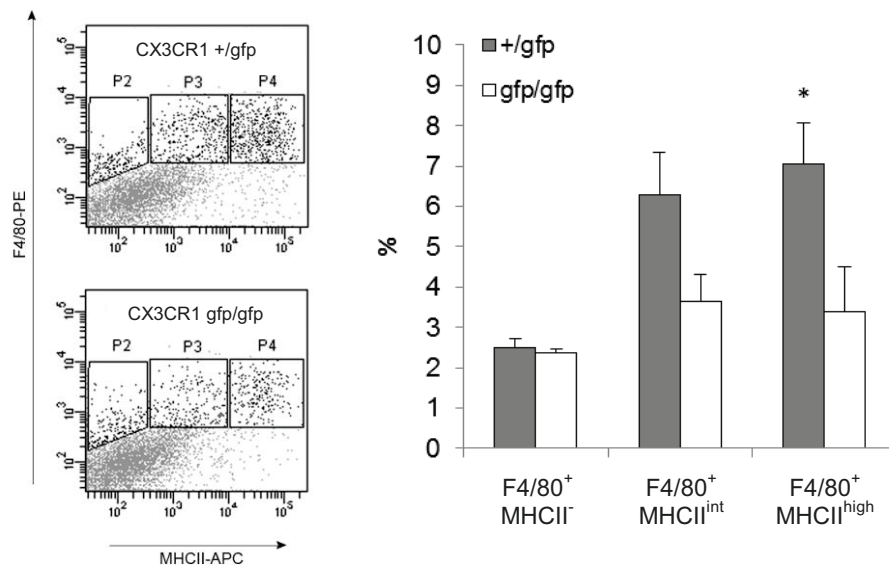


Figure 20. Fractalkine receptor deficiency is associated with reduced macrophage numbers in the white adipose tissue.

Dot plots showing different fat macrophage populations as identified by flow cytometry using mouse specific PE-labelled F4/80 and APC-labelled MHCII antibodies. Quantitative analysis revealed significantly more macrophages in epididymal fat pads of CX3CR1 +/gfp mice, compared to CX3CR1 gfp/gfp animals (two way ANOVA, $p < 0.01$). F4/80⁺ MHCII^{high} cells (P4 gate), but not F4/80⁺ MHCII^{int} cells (P3 gate) or F4/80⁺(low) MHCII⁻ cells (P2 gate) are significantly decreased in response to fractalkine receptor deficiency. * $p < 0.05$, two way ANOVA, followed by Sidak's multiple comparison test, $N = 3$ per group. FatED – fat enriched diet, ND – normal diet.

5.4. Inflammation in adipose tissues is related with the amount of macrophages

5.4.1. Chemokine expression in adipose tissues

Adipocytes express chemokines during the development of obesity, which play important role in recruitment, infiltration and activation of monocytes into various endangered tissues.

CCL2 also contributes to the local proliferation of tissue macrophages. To reveal the importance of these chemokines in accumulation of GFP-positive immune cells to adipose

tissues, I have compared their relative expression in mice exposed to ND or FatED. Chemokine mRNA levels are shown in Fig. 21 (EWAT) and Fig. 22 (BAT).

Fractalkine (*Cx3c1l*) mRNA level was elevated in response to FatED both in WAT and BAT independently of genotype (WAT: diet effect $F(1,12) = 27.53$, $p < 0.001$; BAT: diet effect: $F(1,11) = 33.13$, $p < 0.001$), which suggest that absence of the cognate receptor does not affect the expression of the ligand in the adipose tissues.

However *Ccl2* showed differences in genotype. *Ccl2* expression was over 20 fold higher in both adipose tissues of +/gfp FatED mice, while in gfp/gfp FatED group it was significantly lower (WAT: diet effect: $F(1,14) = 35.89$, $p < 0.001$; genotype effect: $F(1,14) = 15.42$, $p < 0.01$; diet*genotype: $F(1,14) = 14.93$, $p < 0.01$; BAT: diet effect: $F(1,11) = 9.08$, $p < 0.05$; genotype effect: $F(1,11) = 7.99$, $p < 0.05$; diet*genotype: $F(1,11) = 7.89$, $p < 0.05$).

5.4.2. Inflammatory cytokine expression in adipose tissues

Proinflammatory cytokines (M1 markers):

As I have detected significant differences in the number of macrophages in the adipose tissues of mice exposed to FatED, next, I compared the mRNA levels of proinflammatory cytokines produced by macrophages.

In EWAT FatED increased *Il1a*, *Il1b*, *Il6* and *Tnfa* mRNA levels (Fig. 21. diet effect: $F(1,13) = 29.80$, $p < 0.001$, $F(1,13) = 9.17$, $p < 0.01$, $F(1,13) = 6.42$, $p < 0.05$, $F(1,13) = 79.44$, $p < 0.001$, respectively). In gfp/gfp FatED mice *Il1a*, and *Tnfa* levels were significantly lower than in +/gfp fat dieted group. *Il6* mRNA level was lower in gfp/gfp mice (genotype effect: $F(1,12) = 4.71$, $p < 0.05$). Post-hoc analysis did not show differences in mRNA levels.

Because NALP3 inflammasome is critical in processing pre-proIL1 into releasable form, I checked if *Nlrp3* (the gene encoding NALP3) gene expression changed in response to FatED and/or in the absence of fractalkine signaling. As shown in Fig. 21, FatED resulted in elevation of *Nlrp3* mRNA levels in EWAT (diet effect: $F(1,12) = 41.15$, $p < 0.001$). It has also been revealed that FatED induced increase in *Nlrp3* mRNA was significantly lower in fractalkine receptor deficient mice than that of Cx3CR1 +/gfp animals.

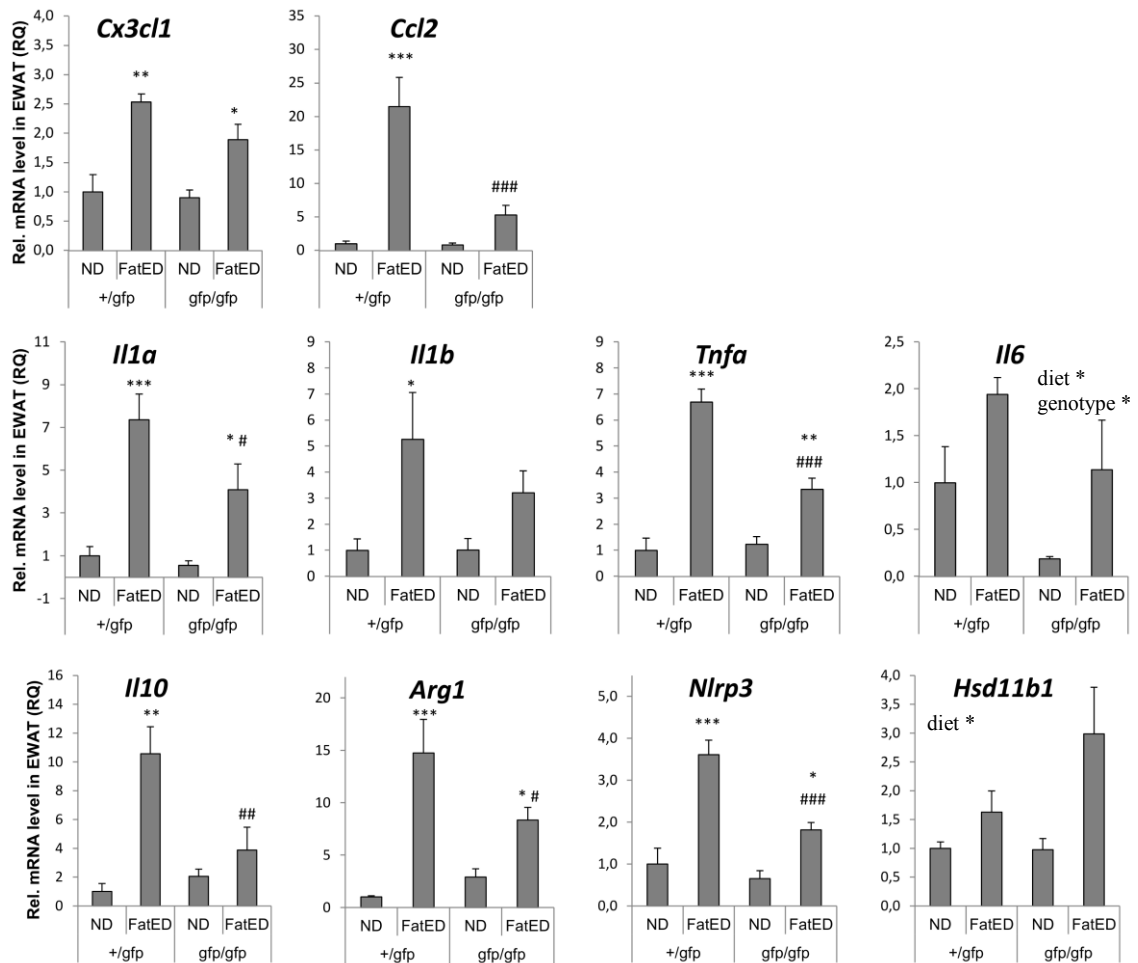


Figure 21. Effect of fat-enriched diet on various markers in EWAT.

Mean \pm SEM values for relative mRNA levels in EWAT. Chemokines: *Cx3cl1*, *Ccl2*;

proinflammatory markers: *Il1a*, *Il1b*, *Tnfa*, *Il6*, *Nlrp3*; anti-inflammatory markers: *Il10*, *Arg1*.

$N = 4-5$ per group. * $p < 0.05$, ** $p < 0.01$, *** < 0.0001 vs. ND, # $p < 0.05$, ## < 0.01 , ### < 0.001 vs. +/gfp (Newman-Keuls post-hoc comparison). FatED – fat enriched diet, ND – normal diet.

FatED upregulated the expression of *Il1a*, *Il1b* and *Tnfa* mRNA levels in BAT (*Il1a*: diet effect: $F(1,11) = 11.93$, $p < 0.01$; *Il1b*: diet effect: $F(1,11) = 19.09$, $p < 0.01$; *Tnfa*: diet effect: $F(1,11) = 23.75$, $p < 0.001$; genotype effect: $F(1,11) = 7.61$, $p < 0.05$) but, according to post-hoc comparison, it was statistically significant only in +/gfp mice, except *Il1b*, where the elevation was almost significant also in gfp/gfp mice ($p = 0.051$). *Il1a* and *Tnfa* levels were significantly lower in gfp/gfp FatED mice compared to +/gfp FatED mice (Fig. 22).

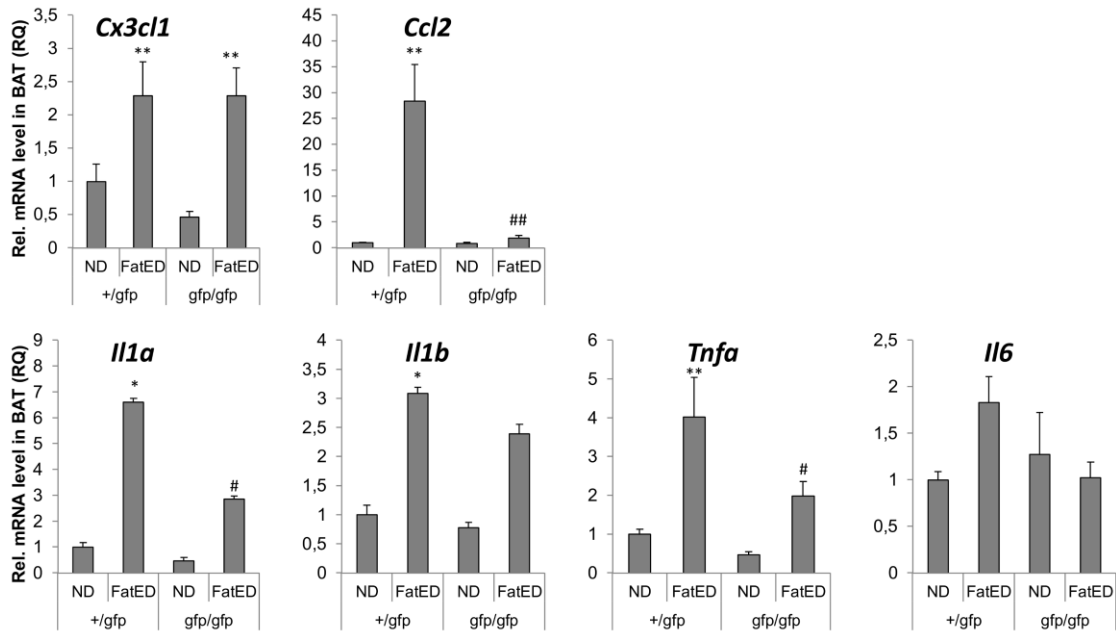


Figure 22. Expression of chemokines and proinflammatory cytokines in BAT.

Mean \pm SEM values for relative mRNA levels in BAT: chemokines: *Cx3cl1*, *Ccl2*; proinflammatory cytokines: *Il1a*, *Il1b*, *Tnfa*, *Il6*. $N = 3-5$ per group. * $p < 0.05$, ** $p < 0.01$ vs. ND, # $p < 0.05$, ## $p < 0.01$ vs. +/gfp (Newman-Keuls post hoc comparison). FatED – fat enriched diet, ND – normal diet.

Anti-inflammatory cytokines (M2 markers):

Alternatively activated macrophages (M2) express set of anti-inflammatory cytokines and mediators involved in tissue restoration. To address changes in select M2 markers during fat-enriched dieting, I measured mRNA levels of *Il10* and *Arg1* in the EWAT. FatED increased *Il10* and *Arg1* mRNA levels (Fig. 21; diet effect: $F(1,12) = 21.08$, $p < 0.001$, $F(1,12) = 25.68$, $p < 0.001$, respectively). In gfp/gfp fractalkin receptor knockout mice, *Il10* and *Arg1* elevation was significantly lower than in +/gfp animals following fat-enriched diet.

Increased levels of *Hsd11b1* mRNA were found in the epididymal WAT in both genotypes ($F(1,14) = 6.92$, $p < 0.05$) as a response to FatED (Fig. 21).

5.5. 10 weeks of FatED does not induce severe inflammation in liver

To investigate whether 10 weeks of FatED induces macrophage accumulation and inflammation in liver, I have measured relative quantities of *Ccl2*, *Cx3cl1*, *Il1a*, *Il1b* and *Il6*, and *Tnfa* mRNA in liver samples of mice from both genotypes after exposure either normal or FatED (Fig. 23). Although *Cx3cl1* expression slightly elevated, *Ccl2* did not change in response to FatED (*Cx3cl1*: diet effect: $F(1,11) = 5.24$, $p < 0.05$). Equal *Gfp* mRNA levels in all groups suggest that macrophages did not accumulate into the liver. Still, elevation in *Il1a*

and *Il6* mRNA expression in FatED groups was found (*Il1a*: diet effect: $F(1,12) = 7.50$, $p < 0.05$; *Il6*: diet effect: $F(1,12) = 7.85$, $p < 0.05$; genotype effect: $F(1,12) = 11.63$, $p < 0.01$), but post-hoc comparison showed significant elevation only in *Il6* in +/gfp mice. *Il1b* and *Tnfa* also showed a slight elevation in response to diet, but it was not significant (*Il1b* diet effect: diet effect: $F(1,12) = 3.83$, $p = 0.07$; *Tnfa* diet effect: $F(1,12) = 3.93$, $p = 0.07$).

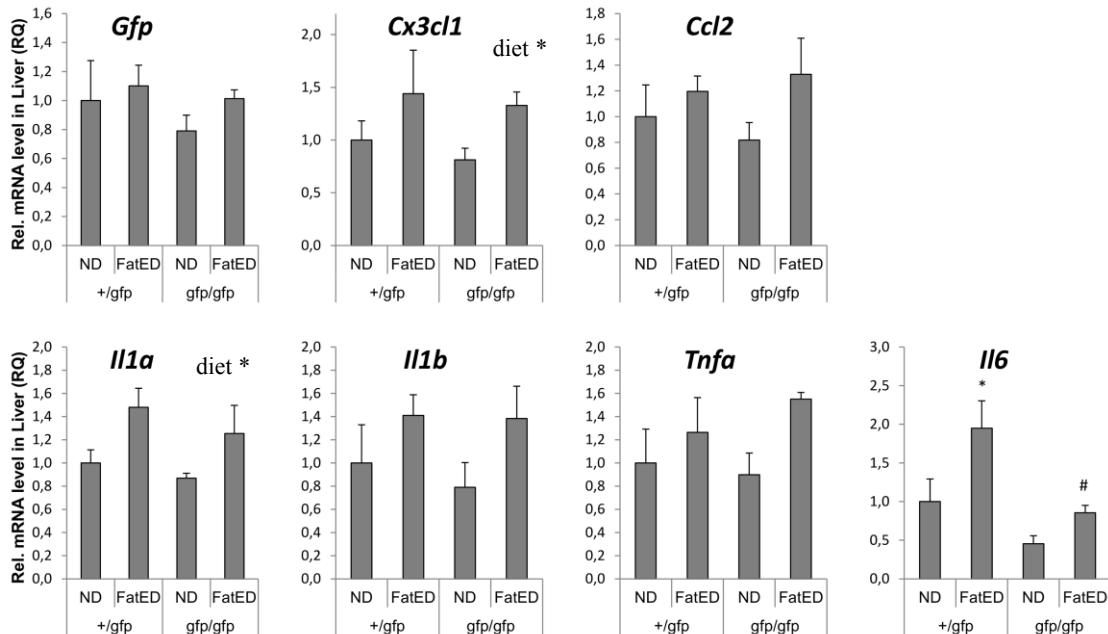


Figure 23. Expression of inflammatory markers in liver.

Mean \pm SEM values for relative mRNA levels in liver. $N = 4-5$ per group. * $p < 0.05$ vs. ND, # $p < 0.05$ vs. +/gfp (Newman-Keuls post-hoc comparison). FatED – fat enriched diet, ND – normal diet.

5.6. 10 weeks of FatED does not induce tissue inflammation in hypothalamus

Inflammatory markers and energy homeostasis regulatory peptides

Neuroinflammation in metabolic-related cell groups of the medial basal hypothalamus has been recently detected in high fat fed rodents and obese humans [44]. Normalized *Gfp* mRNA levels in hypothalamus samples showed significant genotype, diet effect, and genotype*diet interaction: ($F(1,14) = 12.73$, $p < 0.01$; $F(1,14) = 4.70$, $p < 0.05$; $F(1,14) = 16.41$, $p < 0.01$, respectively). Post-hoc analysis revealed increased *Gfp* mRNA level in FatED fed +/gfp mice, but not in gfp/gfp FatED mice.

Relative *Ccl2* mRNA levels were lower in gfp/gfp mice (genotype effect: $F(1,14) = 4.77$, $p < 0.05$) than in the controls (Fig. 24).

There were no significant differences in proinflammatory cytokine mRNA levels (*Il1a*, *Il1b*, *Il6* and *Tnfa*). Although there was a trend towards a decrease in *Il6* mRNA level in CX3CR1 gfp/gfp mice, it was not statistically significant (genotype effect: $F(1,14) = 3.87$, $p = 0.07$).

Among the hypothalamic metabolic-related neuropeptides, FatED feeding decreased the level of orexigenic *Npy* mRNA level (diet effect: $F(1,13) = 16.63$, $p < 0.01$), post-hoc analysis showed significant decrease only in gfp/gfp FatED mice compared to gfp/gfp ND mice.

FatED did not alter anorexigenic *Pomc* mRNA levels (Fig. 24).

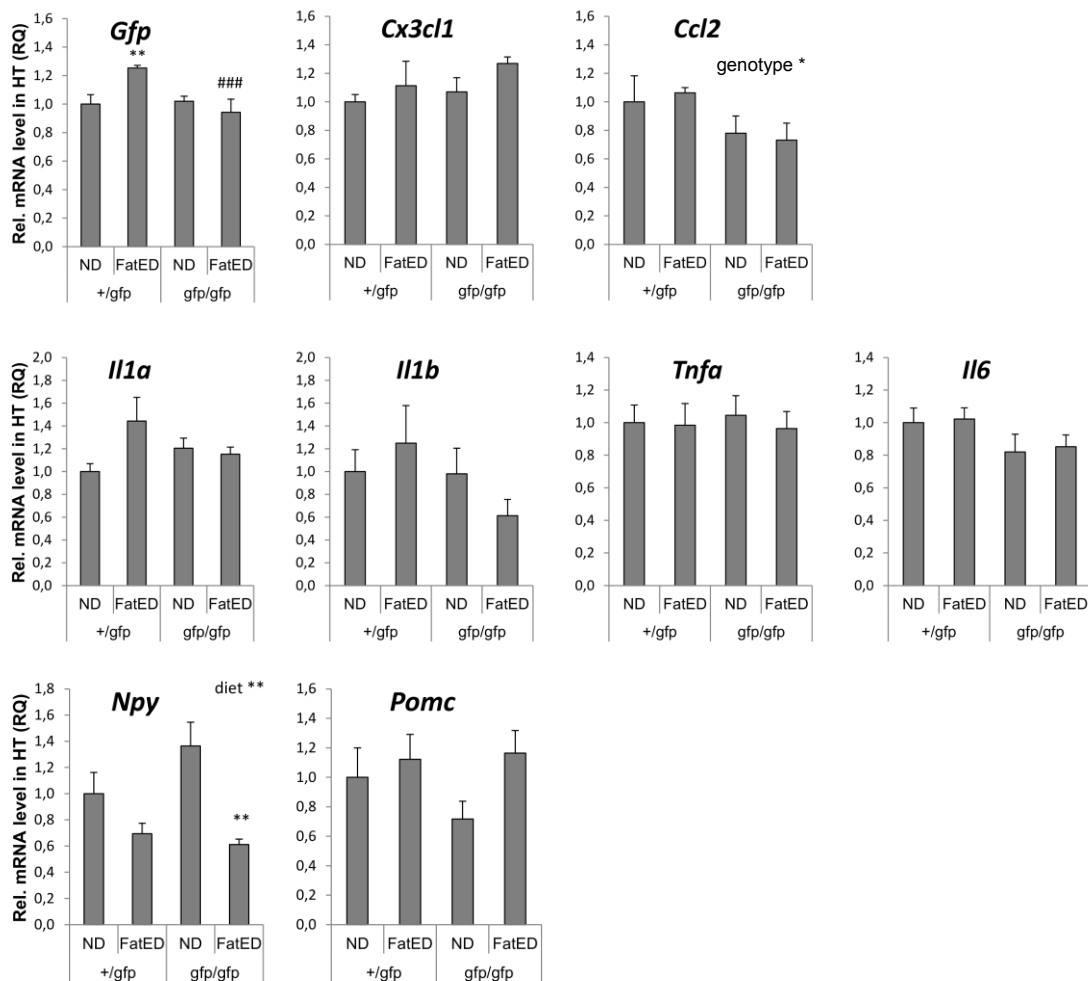


Figure 24. Expression of inflammatory markers and energy homeostasis regulatory peptides in the hypothalamus.

Mean \pm SEM values for relative mRNA levels in hypothalamus. $N = 4-5$ per group. ** $p < 0.01$ vs. ND, ### $p < 0.001$ vs. +/gfp (Newman-Keuls post-hoc comparison). FatED – fat enriched diet, ND – normal diet.

5.7. Fractalkine - CX3CR1 signaling affects lipolysis/lipogenesis balance in BAT

To analyze whether differences in lipid metabolism contribute to diet-induced phenotypic- and morphological changes in BAT of +/gfp and gfp/gfp animals, I have measured expression of enzymes involved in lipid synthesis and lipolysis in the BAT.

FatED upregulated lipogenic enzymes, *Dgat1* and *Gpat* mRNA expression in both genotypes, although elevation in *Dgat1* expression was statistically significant only in gfp/gfp mice, according to post-hoc analysis ($p = 0.07$ between +/gfp groups). There were no statistically significant differences in *Mgat* mRNA levels. Lipolytic enzyme expression (*Atgl*, *Hsl*, *Mgl*) did not change in response to FatED in +/gfp mice. Gfp/gfp ND fed mice express lower levels of *Atgl* and *Mgl* than +/gfp ND mice, and FatED upregulated all lipolytic enzymes' mRNA expression (Fig. 25) (Lipogenic enzymes: *Dgat1* (diet effect: $F(1,13) = 76.94$, $p < 0.001$); *Gpat* (diet effect: $F(1,13) = 129.54$, $p < 0.001$; diet * genotype: $F(1,13) = 12.44$, $p < 0.01$). Lipolytic enzymes: *Atgl* (diet effect: $F(1,13) = 22.12$, $p < 0.001$; diet * genotype: $F(1,13) = 6.64$, $p < 0.05$); *Hsl* (diet effect: $F(1,13) = 18.02$, $p < 0.001$; diet * genotype: $F(1,13) = 20.04$, $p < 0.001$); *Mgl* (diet effect: $F(1,13) = 32.10$, $p < 0.001$; diet * genotype: $F(1,13) = 9.07$, $p < 0.05$)).

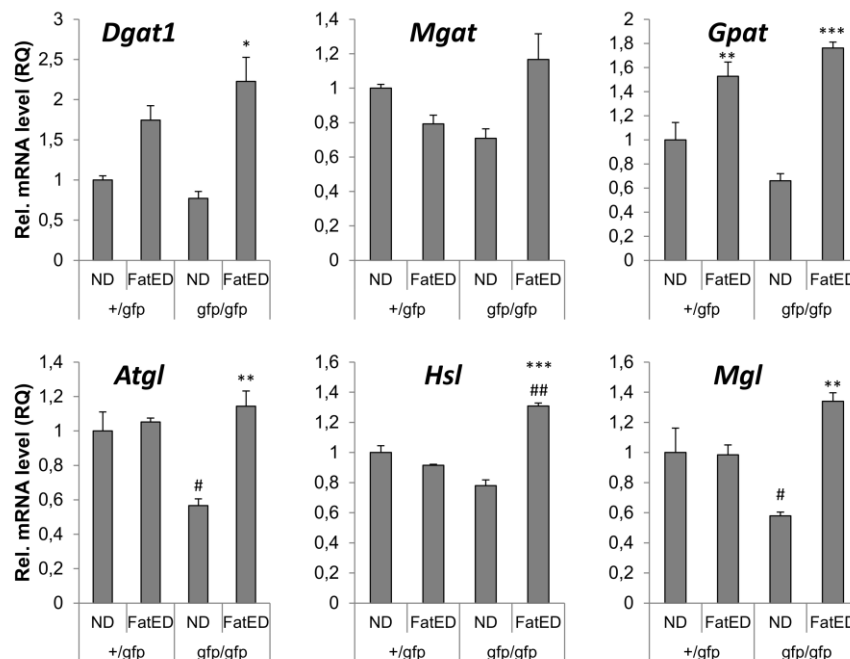


Figure 25. Gene expression of lipogenic and lipolytic enzymes in the BAT.

Lipogenic enzymes: top row, lipolytic enzymes, bottom row. Mean \pm SEM values for relative mRNA levels in BAT. $N = 4-5$ per group. * $p < 0.05$, ** $p < 0.01$, *** $p < 0.0001$ vs. ND, # $p < 0.05$, ## $p < 0.01$ vs. +/gfp (Newman-Keuls post hoc comparison). FatED – fat enriched diet, ND – normal diet.

5.8. Fractalkine – CX3CR1 signaling affects the expression of BAT thermogenic and metabolic-related markers

Because BAT significantly contributes to energy expenditure via non-shivering thermogenesis by using fatty acids and glucose as fuels, next I investigated the diet-induced expression of thermogenesis-related markers in the BAT of mice with or without fractalkine signaling.

In +/gfp mice, fat enriched diet did not affect expression of *Ucp1*, *Pparg2* and *Pgc1a*, however, *Dio2* and *Adrb3* mRNA levels were elevated. Gfp/gfp mice express less *Ucp1*, *Pparg2* and *Pgc1a* mRNA, than +/gfp mice under normal diet, exposure to FatED resulted in significantly elevated expression of these mRNAs in the BAT. *Pparg2* and *Adrb3* mRNA levels in gfp/gfp FatED mice was higher than in +/gfp FatED mice (Fig. 26) (*Ucp1*: diet effect: $F(1,11) = 23.68$, $p < 0.001$; genotype * diet: $F(1,11) = 13.74$, $p < 0.01$; *Pparg2*: diet effect: $F(1,11) = 26.88$, $p < 0.001$, genotype * diet: $F(1,11) = 43.91$, $p < 0.001$; *Pgc1a*: diet effect: $F(1,11) = 15.74$, $p < 0.01$; genotype * diet: $F(1,11) = 7.75$, $p < 0.05$. *Dio2*: diet effect: $F(1,11) = 24.70$, $p < 0.001$; genotype effect: $F(1,11) = 17.35$, $p < 0.01$. *Adrb3*: diet effect: $F(1,11) = 89.78$, $p < 0.001$; genotype effect: $F(1,11) = 7.56$, $p < 0.05$; genotype * diet: $F(1,11) = 28.23$, $p < 0.001$).

Because adipose tissue macrophages synthesize and release catecholamines locally in response to cold [90], I have been interested how tyrosine hydroxylase (*Th*), the key enzyme in catecholamine synthesis, varies in the BAT in response to diet. Neither the genotype nor the diet affected *Th* mRNA expression in the BAT.

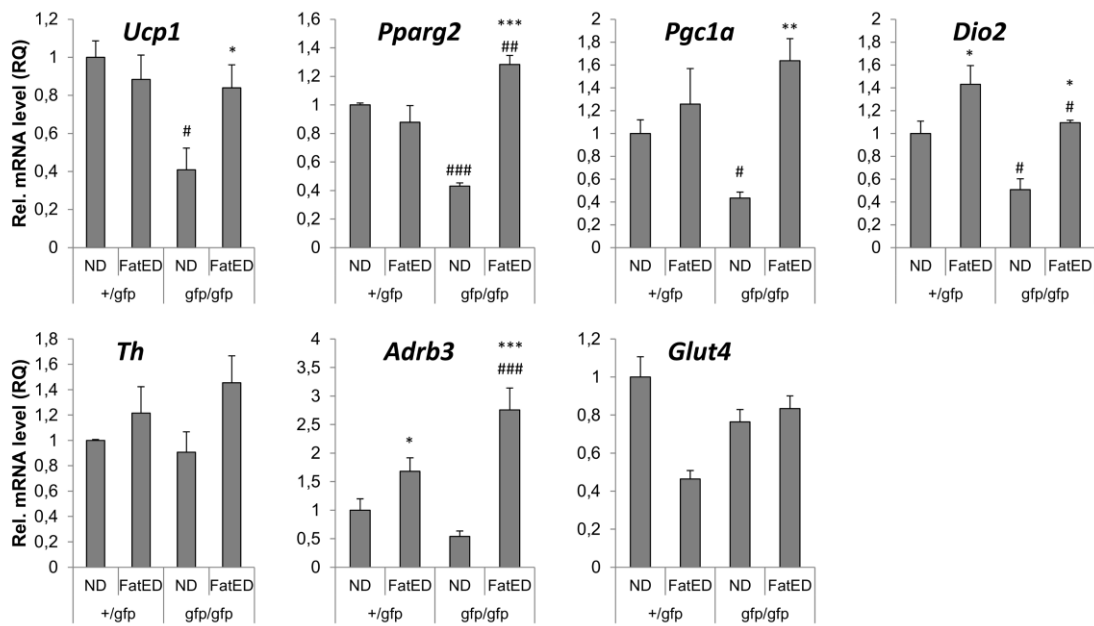


Figure 26. Gene expression of BAT thermogenic and metabolic-related markers.

Mean \pm SEM values for relative mRNA levels in BAT. $N = 4-5$ per group. * $p < 0.05$, ** $p < 0.01$, *** $p < 0.001$ vs. ND; # $p < 0.05$, ## $p < 0.01$, ### $p < 0.001$ vs. +/gfp (Newman-Keuls post hoc comparison). FatED – fat enriched diet, ND – normal diet.

5.9. FatED results in elevated UCP1 protein levels in fractalkine deficient mice

Using Western blot analysis I showed that FatED did not change UCP1 protein levels in +/gfp FatED mice. On the contrary, FatED resulted in elevated UCP1 levels in gfp/gfp animals (Fig. 27). The difference seen in *Ucp1* mRNA levels between ND groups was not recognized at protein level.

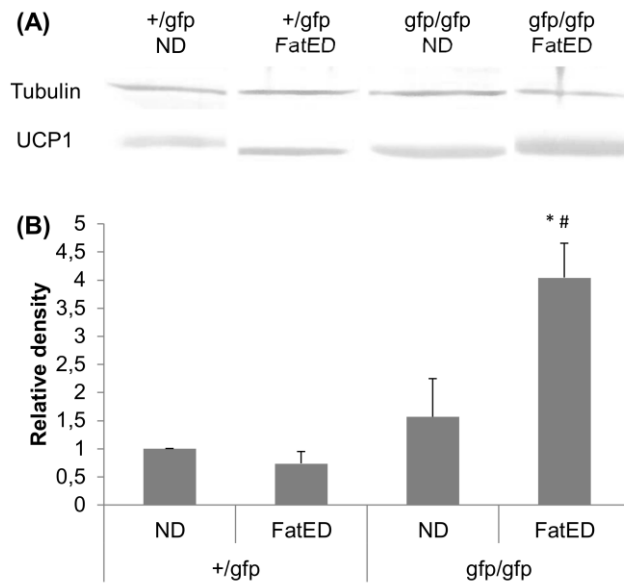


Figure 27. UCP1 protein levels in BAT. A) Representative Western blot image. B) Mean \pm SEM values for relative density of UCP1 in BAT. $N = 3$ per group. * $p < 0.05$ vs. ND; # $p < 0.05$ vs. +/gfp (Newman-Keuls post hoc comparison). FatED – fat enriched diet, ND – normal diet.

6. Discussion

Present results show the importance of fractalkine – CX3CR1 signaling in the development of obesity. Mice with normal fractalkine signaling (CX3CR1 +/gfp) on FatED gain significant body weight by storing excess fat in the adipose tissues. Not only the hypertrophy of white adipocytes in EWAT and SWAT was observed, but remodeling and “whitening” of BAT. Adipocyte hypertrophy was associated with recruitment of macrophages, formation of CLS and expression of inflammatory cytokines both in WAT and BAT. Because of the remodeling and inflammatory environment, thermogenesis in BAT was impaired, therefore the decreased energy expenditure and the elevated fat intake and storage led to obesity, chronic low grade inflammation, glucose intolerance and cold intolerance. Lack of fractalkine signaling prevented macrophage accumulation into adipose tissues and consequently, the inflammatory cytokine expression. Furthermore, with the lack of macrophages and inflammation, thermogenic capacity in BAT was upregulated, therefore the elevated energy expenditure could compensate the increased fat intake, and decrease body weight gain.

High fat diet is a major environmental factor that triggers obesity both in humans and in rodents [91]. There are several diets and paradigms to induce obesity. Among these, I used fat-enriched food which has been shown to be a relevant trigger for obesity and related pathologies [92-95]. To exclude any food preference, a mixture of chow and lard was given. Heterozygous (CX3CR1 +/gfp) FatED animals with intact fractalkine signaling started to gain more weight than mice on ND and the difference in body weight became significant after week 5. This time course is comparable to those obtained after various high fat diets [96-100]. By contrast, mice - in which fractalkine signaling is compromised -, gain much less weight when on fat-enriched diet than heterozygotes (even though their energy intake and fecal output was equal). These results and the normal glucose tolerance and plasma cytokine levels suggest that CX3CR1 gfp/gfp mice are somehow resistant to diet-induced obesity.

In heterozygote (CX3CR1 +/gfp) mice, changes in body weight were accompanied with increases in body fat depots. Notably, EWAT and BAT was also enlarged in CX3CR1 gfp/gfp mice, but the increase was significantly less than that seen in animals with +/gfp genotype. My results on diet-induced obesity in CX3CR1 gfp mice differ from other reports on this model. For instance, Morris et al [73] and Lee et al [101] and Shah et al [102] failed to detect differences in HFD induced body weight and adiposity in fractalkine receptor KO mice and controls. These discrepancies might be due to the different composition of high fat diet (20% protein, 20% carbohydrate and 60% fat for Morris and Lee; 20% protein, 35% carbohydrate, 45% fat for Shah; 9,7% protein, 28% carbohydrate and 62,3% fat in my studies), duration of

the diet (30 weeks for Morris, 24 weeks for Lee, 4-24 for Shah and 10 weeks in this study), different hygienic status of the animal facility (SPF for Morris and Shah, MD in my studies), or strain differences (CX3CR1KO for Lee vs. CX3CR1gfp in my studies). The hygienic status of the animal facility might be important in DIO models, as gut microbiota plays pivotal role in the development of obesity [103-105]. Moreover, in a study comparing DIO in conventional and SPF animal facilities, only conventional DIO mice were characterized by metabolic endotoxemia and low-grade inflammation [106].

Activity of the hypothalamo-pituitary-adrenocortical axis in general, and corticosterone plasma levels in particular have been shown to contribute to regulation of abdominal fat deposition [92, 107]. Data on high fat diet-induced corticosterone concentrations are highly controversial: there are reports on increase, decrease or unchanged levels (see [108] for review). Here I found a tendency for FatED-induced adrenocortical hyperactivity in both genotypes. At cellular level, corticosteroid action is dependent on the activity of type 1, 11 β -hydroxysteroid dehydrogenase (HSD11B1) which converts inactive corticosteroids into active corticosterone in mice. In contrast to previous view [109], recent data support the main effect of high fat diet-induced adipose specific HSD11B1 downregulation promoted fat accumulation [110]. Furthermore, high local concentration of corticosterone in adipose tissue and/or elevated plasma concentration in CX3CR1 gfp/gfp mice might reduce macrophage production of proinflammatory cytokines and promote anti-inflammatory responses [111].

Both type of adipose tissue displays significant morphological and functional plasticity driven by metabolic-, environmental- and hormonal cues [112]. “Browning” of the white adipose tissue is well recognized. For instance, clusters of UCP1 expressing cells referred to as “brite” (brown in white or beige) adipocytes appear in the white adipose tissue in response to cold, while there is a downregulation of *Ucp1* mRNA levels together with phenotypic appearance of white adipocytes in the BAT at thermoneutral conditions [113]. Here I have shown „whitening” of BAT in response to fat-enriched diet in mice, which is due to coalescence of lipid droplets. Similar, distorted lipid droplet architecture has also been reported in mice kept on high fat diet for 13 weeks [114, 115]. Increase of the size of lipid droplets might indicate an imbalance between lipid synthesis and lipolysis. Indeed, present results show that lipogenic enzymes expression were upregulated in both FatED groups, while lipolytic enzymes were upregulated only in gfp/gfp mice, which might be responsible for less fat deposition in BAT of these animals.

Analysis of resident macrophage population in the white adipose tissue of intact animals revealed significantly less macrophages with F4/80+MHCII high phenotype in CX3CR1 *gfp/gfp* animals than in CX3CR1 *+gfp* heterozygotes.

In addition to morphological changes of adipocytes I found recruitment/accumulation of mononuclear cells into the WAT and BAT of *+gfp* mice kept on fat-enriched diet. Number of CLS is a good indicative of the infiltrated macrophages in WAT as > 90% of them are found in these structures [89]. In EWAT of obese *+gfp* animals significantly higher number of CLS was found than in CX3CR1 *gfp/gfp* mice on FatED. CLS formation in the SWAT of FatED fed mice was not significant, which is in accordance with other experiments, where CLS were less prevalent in subcutaneous than in visceral fat [116]. However CLS in BAT is not documented. I found CLS – similar to those found in the EWAT of obese animals - surround enlarged BAT cells with distorted lipid droplets. Beyond the immunohistochemical analysis of CLS, I confirmed macrophage accumulation by qPCR measurement of *Gfp* mRNA in the tissues. Fat-enriched diet resulted in an increase of normalized *Gfp* mRNA expression in the EWAT, BAT, liver and hypothalamus in animals with intact fractalkine signaling, indicative of selective recruitment and/or activation of cells expressing CX3CR1/*gfp*. Indeed, obesity induces infiltration of macrophages into the epididymal fat, the adipose tissue macrophage content correlates with the measures of obesity and cytokines released from these cells contribute to the insulin resistance of the adipocytes [40, 117].

These data are also consistent with previous results showing that genetic and diet-induced obesity results in chronic inflammation in the BAT [118-120]. By contrast, Fitzgibbons et al. found very low level of immune cell enriched transcripts in the BAT from C57BL6/J mice fed a high-fat diet for 13 weeks [114]. Thus the extent of BAT inflammation is largely depends on the strain and conditions used.

Recruitment of leukocytes into the white adipose tissue and their role in metabolic inflammation is well recognized both in genetic- and diet-induced rodent models as well as in human obesity [121]. Feeding a high fat diet to C57Bl6 mice has been shown to promote large increases of various leukocytes, among those T cells and neutrophils are the first on the scene, followed by monocytes/macrophages by 8-10 weeks on diet [122]. Adipose tissue macrophages have been mechanistically implicated in low grade, long lasting, metabolic inflammation and glucose intolerance seen in diet-induced obesity [117, 123]. It has been hypothesized that dying adipocytes initiate macrophage recruitment to the adipose tissue, however, recent findings emphasize the role of various chemokines originating from adipocytes and/or from the stromal vascular fraction. In this respect the monocyte attractant protein, CCL2 (MCP1) and its receptor CCR2 have been the most intensively studied [124].

Although *Mcp1* mRNA level in the adipose tissue is elevated within 7 days and plasma MCP1 concentration increased 4 weeks after starting high fat diet, genetic disruption of MCP1 signaling did not confer resistance to diet-induced obesity in mice or reduce adipose tissue macrophage infiltration in the WAT [124], indicating involvement of additional monocyte attractants.

One interesting finding of the present study is the lack of diet-induced elevation of *Ccl2* (*Mcp1*) in fractalkine receptor deficient mice, suggesting some mechanistic relationship between these chemokines.

Recent results of Shah et al in humans [56] demonstrated that fractalkine (CX3CL1) is significantly increased in obesity and revealed adipocytes and stromal vascular fraction as source of this adipochemokine that mediates monocyte adhesion to human adipocytes. Fractalkine is implicated in recruitment of leukocytes in clinical syndromes of adipose tissue inflammation and atherosclerosis. Here I have confirmed upregulation of fractalkine transcription in the adipose tissue of mice on fat-enriched diet and identified the fractalkine receptor CX3CR1 as an important mediator of monocyte/macrophage recruitment into the visceral fat in obesity. Furthermore I reported, for the first time, that fat enriched diet induces fractalkine expression in brown adipose tissue as well. This scenario shows similarities with mouse models of atherosclerosis, where disruption of either CX3CL1 or CX3CR1 attenuates macrophage trafficking and inflammation [125-127]. By contrast, Morris et al did not find differences in total adipose tissue macrophages (ATM), in the ratio of type 1 (CD11c(+)) to type 2 (CD206(+)) ATMs, expression of inflammatory markers, and T-cell content in epididymal fat from obese CX3CR1(+/*gfp*) and CX3CR1(*gfp/gfp*) mice [73]. Beside the differences in housing and dieting conditions, these discrepancies raise a relevant possibility that cells attracted to the adipose (target) tissue downregulate their special surface markers.

Based on the facts that expression of fractalkine has been significantly elevated in all groups fed with FatED, while mice lacking the fractalkine receptor accumulated significantly less GFP+ cells into the BAT and display less severe local tissue inflammation than controls, I propose a role of fractalkine/fractalkine receptor system in recruitment of macrophages into the BAT.

CLS are regarded as a major source of proinflammatory cytokines in the inflamed fat tissue. Indeed, my data demonstrate upregulation of proinflammatory cytokines *Il1a*, *Il1b* and *Tnfa* expression in the EWAT and BAT of control mice (CX3CR1 +/*gfp*) in response to fat-enriched diet. This effect was attenuated in CX3CR1 *gfp/gfp* mice, supporting the hypothesis that fractalkine signaling is involved in the activation/polarization of adipose tissue macrophages in obesity [95, 117]. However, the specific leukocyte/macrophage population,

which contributes to the local elevation of proinflammatory cytokines in the fat challenged adipose tissue, remains to be elucidated.

Processing of pro IL1b by the NLRP3 inflammasome has recently been implicated in obesity [128]. Here I have revealed an increase of *Nlrp3* mRNA within the epididymal fat pad of CX3CR1 +/gfp mice fed with fat-enriched diet that might contribute to an elevated tissue levels of *Il1b*. There are several danger-associated signals that might induce assembly of NLRP inflammasome and sterile inflammation of the visceral fat in obese subjects. For instance, ceramide and palmitate have been implicated in activation and /or priming of the inflammasome in adipose tissue and macrophages [129].

Accumulation of proinflammatory macrophages in obese adipose tissues shows similarities to foam cell formation in atherosclerotic plaques, which is also dependent on the presence of CX3CR1 [125]. It should be recognized, however, that different subsets of monocytes use different chemokine patterns with which to accumulate in various inflammatory targets [130].

It has been shown previously that adipose tissue macrophages in lean animals express markers characteristic of alternatively polarized (M2) macrophages, while high fat diet-induced obesity results in a phenotypic change to M1 polarization [41].

In addition to proinflammatory cytokines, I have demonstrated significant upregulation of two anti-inflammatory markers *Il10* and *Arg1* mRNA in WAT samples from CX3CR1 +/gfp animals kept on fat-enriched diet, which can be interpreted as a local compensatory mechanism [131, 132]. It should be noted however, that neither baseline expression, nor diet-induced upregulation of *Il10* and *Arg1* transcription is significant in mice with impaired fractalkine signaling.

Among the cytokines induced by FatED in the BAT, TNFa might play a prominent role in morphofunctional rearrangements. For instance, TNFa decreased the expression of functionally active ADRB3 receptors in brown adipocytes and consequently attenuated the thermogenic and lipolytic actions of sympathetic nervous system (SNS) activity [133]. Studies on 3T3-L1 adipocytes revealed that TNFa attenuates expression of lipolytic enzymes *Atgl* and *Hsl* [134]. Conversely, TNFa deficiency in genetically obese (ob/ob) mice resulted in less severe obesity, decrease in brown adipocyte apoptosis, and increased expression of *Adrb3* and *Ucp1* with significant improvement of thermogenetic capacity [133]. Fractalkine receptor deficient mice (gfp/gfp), in which FatED- did not induce local *Tnfa* expression, are protected from excessive weight gain, display improved glucose tolerance and induction of *Adrb3*, *Atgl* and *Hsl* mRNA in the BAT.

The next obvious question was how FatED-induced proinflammatory environment affects energy expenditure/cold tolerance and BAT expression of metabolic-related and thermogenic genes. CX3CR1 +/gfp mice do not increase BAT expression of *Ucp1*, *Pparg2*, and *Pgc1a* in

response to FatED, which might explain their obesity prone phenotype and impaired cold tolerance during fat enriched diet. Indeed, it has been recently shown that macrophage derived proinflammatory cytokines in general-, and TNF α in particular, suppress the induction of *Ucp1* promoter activity and mRNA expression [135, 136]. Diet-induced differences of UCP1 protein in the BAT of +/gfp and gfp/gfp of mice has been confirmed at protein level, however the mismatch seen in normal dieted mice between *Ucp1* mRNA, UCP1 protein levels and cold tolerance might be related to different mRNA stability and/or differences in the hormone/cytokine milieu and needs further investigation. By contrast, it is interesting to recognize that *Dio2* expression was slightly increased in the BAT of obese FatED +/gfp mice. Increased DIO2 activity would have resulted in elevated local levels of T3 and induce UCP-driven thermogenesis. Nevertheless, the interaction between various hormonal- (T3, corticosteroids, insulin) autonomic- (sympathetic drive) and inflammatory cytokines and adipocytes is quite complex and occurs at several functionally distinct loci of obesity.

Present data demonstrate that fat-enriched diet-induced proinflammatory cytokine expression is limited to the adipose tissues, because *Il1a*, *Il1b* and *Tnfa* mRNA levels did not change in the liver and in the hypothalamic samples. In contrast, Thaler et al [44] reported a HFD-induced bi-phasic hypothalamic inflammation in rats, the first occurs shortly after starting the diet and the second observed in response to chronic HFD exposure. It remains unknown whether our fat-enriched diet is less obesogenic/immunogenic than other high fat diets and/or the length of the exposure was insufficient to induce widespread central inflammation. For instance, ApoE $^{-/-}$ mice kept on highly atherogenic cholate/cholesterol rich diet (Paigen) lose weight and develop vascular inflammation, microglial activation, and leukocyte recruitment in the brain, while those mice that are on fatty Western style diet gain weight and show 57% lower vascular inflammation in the brain [137].

Among the hypothalamic energy homeostasis regulating peptides, the expression of orexigenic *Npy* decreased in FatED fed mice, which can be regarded as compensatory mechanisms to defend body weight. Inhibition of *Npy* and *Agrp* expression is also observed in response to leptin and insulin, which are long-term adiposity signals [138-140]. Nevertheless *Pomc* expression did not change in response to FatED.

In summary, I report that mice with impaired fractalkine signaling are protected from fat-enriched diet-induced obesity. The mechanism might involve altered lipolysis/lipogenesis balance in adipose tissues and altered thermogenesis as a result of impaired recruitment of leukocytes/monocytes to adipose tissues.

These results suggest also that diet-induced recruitment of macrophages in the BAT of +/gfp mice through the release of proinflammatory cytokines like TNF α , results in local

inflammation and may attenuate the sympathetic nervous system (SNS) induced thermogenesis and lipolysis in adipose tissues, leading to fat accumulation, driving a vicious circle. However, impaired fractalkine signaling (in *gfp/gfp* mice) breaks this circle by attenuating the accumulation of adipose tissue macrophages and their cytokine production, which results in diet-induced upregulation of *Atgl*, *Hsl* and *Mgl* lipolytic enzymes and *Ucp1* mRNA and protein in the BAT. These changes are likely to contribute to the improved thermoadaptive response and the leaner phenotype seen in fractalkine receptor deficient mice (Fig.28).

These results open new avenues for CX3CR1 antagonists to fight obesity and metabolic inflammation-related pathologies.

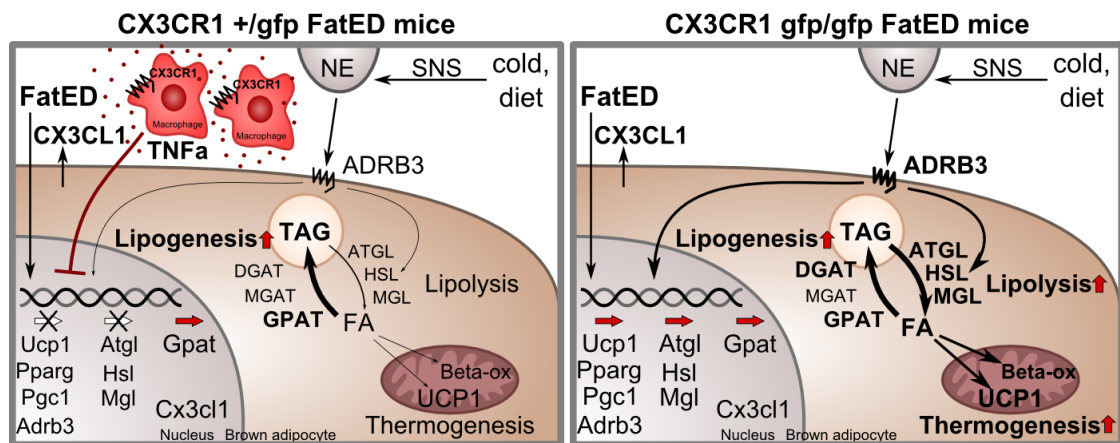


Figure 28. Fractalkine and CX3CR1 contributes to the accumulation of macrophages into BAT during the development of obesity. The presence of macrophages leads to elevated expression of proinflammatory cytokines, which attenuate the thermogenic capacity of BAT.

7. New scientific results

Thesis I.

I have shown that FatED induced obesity and metabolic inflammation is associated with elevated fractalkine expression in WAT and BAT

I have found that

- 10 weeks of fat enriched diet (FatED) results in increased body weight gain in mice.
- Body weight gain/obesity is due to increased fat deposition
- Obese mice display glucose and cold intolerance.
- FatED results in morphological rearrangements and recruitment of leukocytes/macrophages in white and brown adipose tissue depots.
- Obese mice have metabolic inflammation with
 - increased plasma levels of proinflammatory cytokine IL1b;
 - increased mRNA levels of chemokines in white and brown adipose tissue;
 - elevated local expression of proinflammatory cytokines in the WAT and BAT.
- I have shown for the first time that FatED results in fractalkine mRNA induction in the BAT;
- FatED-induced inflammation was localized in the adipose tissues but not seen in the liver or in the hypothalamus.

Thesis II.

I have shown that fractalkine – CX3CR1 signaling contributes to the development of obesity

Because fractalkine-fractalkine receptor system is involved in the signaling, trafficking, recruitment and activation of various leukocytes at the site of inflammation, I have investigated its involvement in metabolic inflammation.

I have provided new evidence that mice with targeted disruption of the fractalkine receptor (CX3CR1) gene (CX3CR1 *gfp/gfp*)

- are less sensitive to obesogenic effect of FatED;
- gain less weight on FatED and do not develop glucose intolerance during the diet;
- their adipocytes are smaller and display significantly less crown like structures in the epididymal WAT and BAT;
- have equally increased expression of fractalkine, but decreased *Ccl2* expression;

- recruit much less GFP+ and F4/80+ macrophages in the WAT and BAT when kept on FatED;
 - display attenuated expression of proinflammatory cytokines in the epididymal WAT and BAT;
 - do not develop serious metabolic inflammation –
- compared to CX3CR1 heterozygotes, which have intact fractalkine signaling.

Thesis III.

I have shown that obesity associated fractalkine – CX3CR1 dependent macrophage infiltration and inflammation in BAT affects thermogenesis

I have found that the obesity resistant phenotype of fractalkine receptor deficient mice is mechanistically associated with

- increased lipolysis due to diet-induced expression of lipolytic - and unchanged lipogenic enzymes;
 - and increased expression of uncoupling protein (UCP1) in the BAT –
- which was not seen in obese mice with normal fractalkine signaling.

8. Possible applications

My new scientific results contribute to the understanding of the development of obesity, metabolic inflammation and control of thermogenesis in BAT. Using this knowledge, new potential therapeutic targets can be identified. First of all, pharmacological inhibition of fractalkine receptor by CX3CR1 antagonist could reduce macrophage accumulation to adipose tissues, therefore reduce adipose tissue inflammation and the development of obesity. Treatment with F1, a CX3CR1 antagonist, has been shown to reduce macrophage accumulation in the aortic sinus in mouse models of atherosclerosis [141], thus its use in obesity is promising. Based on my research, though a CX3CR1 antagonist could prevent the development of obesity if it is administered from onset, it requires further investigation whether it could reduce obesity when it is administered in advanced state. Second, BAT, as an important contributor of energy expenditure by non-shivering thermogenesis, could be a potential therapeutic target. Preventing macrophage accumulation thus preventing proinflammatory cytokine expression in BAT, or blocking the proinflammatory cytokine expression in BAT could upregulate the thermogenic machinery therefore the elevated thermogenic activity could modulate energy intake/energy expenditure balance leading to the utilization of excess fat. In an experiment in mice it has been shown that cold exposure rapidly promotes alternative activation of adipose tissue macrophages, which secrete catecholamines to induce thermogenic gene expression in BAT and lipolysis in WAT [90]. My results suggest that the proinflammatory environment is responsible for the impaired thermogenesis in obese animals. Accordingly setting a cold therapy protocol in humans, which could induce switching of macrophages from proinflammatory to alternatively activated state, could activate BAT thermogenesis in obese people potentially leading to weight loss.

9. Acknowledgement

I would like to thank my supervisor Krisztina Kovács for guiding and supporting me over the years.

Many thanks to my colleagues: Julianna Benkő, Ádám Dénes, Szilamér Ferenczi, Rókus Kriszt, Dóra Kővári, Dániel Kuti, Bernadett Küblerné Pintér, Zsuzsanna Winkler for their help.

I am grateful to the Doctoral School, especially to Dr. Péter Szolgay for the opportunity to participate in the doctoral program, and Tivadarné Vida for her kind help.

I would like to thank my family and friends for supporting me.

The work was supported by grants from Hungarian Research Fund OTKA 109622 to Krisztina Kovács; 109744 to Szilamér Ferenczi and 109743 to Ádám Dénes.

10. References

- 1 <http://www.who.int/mediacentre/factsheets/fs311/en/>
- 2 O'Neill, S., and O'Driscoll, L.: 'Metabolic syndrome: a closer look at the growing epidemic and its associated pathologies', *Obes Rev*, 2015, 16, (1), pp. 1-12
- 3 Monteiro, R., and Azevedo, I.: 'Chronic inflammation in obesity and the metabolic syndrome', *Mediators Inflamm*, 2010, 2010
- 4 https://www.cdc.gov/healthyweight/assessing/bmi/adult_bmi/, accessed 2016.09.09
- 5 Morton, G.J., Meek, T.H., and Schwartz, M.W.: 'Neurobiology of food intake in health and disease', *Nature Reviews Neuroscience*, 2014, 15, (6), pp. 367-378
- 6 Rosenbaum, M., and Leibel, R.L.: 'Adaptive thermogenesis in humans', *Int J Obesity*, 2010, 34, pp. S47-S55
- 7 Gao, Q., and Horvath, T.L.: 'Neurobiology of feeding and energy expenditure', *Annu Rev Neurosci*, 2007, 30, pp. 367-398
- 8 Dietrich, M.O., and Horvath, T.L.: 'Hypothalamic control of energy balance: insights into the role of synaptic plasticity', *Trends Neurosci*, 2013, 36, (2), pp. 65-73
- 9 Loh, K., Herzog, H., and Shi, Y.C.: 'Regulation of energy homeostasis by the NPY system', *Trends in endocrinology and metabolism: TEM*, 2015, 26, (3), pp. 125-135
- 10 Richard, D.: 'Cognitive and autonomic determinants of energy homeostasis in obesity', *Nature reviews. Endocrinology*, 2015, 11, (8), pp. 489-501
- 11 Seoane-Collazo, P., Ferno, J., Gonzalez, F., Dieguez, C., Leis, R., Nogueiras, R., and Lopez, M.: 'Hypothalamic-autonomic control of energy homeostasis', *Endocrine*, 2015, 50, (2), pp. 276-291
- 12 E. Schlenker, J.A.G.: 'Williams' Essentials of Nutrition and Diet Therapy' (Elsevier, 2014, 11th edn. 2014)
- 13 Spiegelman, B.M., and Flier, J.S.: 'Obesity and the regulation of energy balance', *Cell*, 2001, 104, (4), pp. 531-543
- 14 Saely, C.H., Geiger, K., and Drexel, H.: 'Brown versus White Adipose Tissue: A Mini-Review', *Gerontology*, 2012, 58, (1), pp. 15-23
- 15 Pfeifer, A., and Hoffmann, L.S.: 'Brown, Beige, and White: The New Color Code of Fat and Its Pharmacological Implications', *Annu Rev Pharmacol*, 2015, 55, pp. 207-227
- 16 Henry, S.L., Bensley, J.G., Wood-Bradley, R.J., Cullen-McEwen, L.A., Bertram, J.F., and Armitage, J.A.: 'White adipocytes: More than just fat depots', *Int J Biochem Cell B*, 2012, 44, (3), pp. 435-440

- 17 Cannon, B., and Nedergaard, J.: 'Brown adipose tissue: function and physiological significance', *Physiol Rev*, 2004, 84, (1), pp. 277-359
- 18 Bartelt, A., Bruns, O.T., Reimer, R., Hohenberg, H., Ittrich, H., Peldschus, K., Kaul, M.G., Tromsdorf, U.I., Weller, H., Waurisch, C., Eychmuller, A., Gordts, P.L., Rinninger, F., Bruegelmann, K., Freund, B., Nielsen, P., Merkel, M., and Heeren, J.: 'Brown adipose tissue activity controls triglyceride clearance', *Nat Med*, 2011, 17, (2), pp. 200-205
- 19 Peirce, V., and Vidal-Puig, A.: 'Regulation of glucose homeostasis by brown adipose tissue', *Lancet Diabetes Endocrinol*, 2013, 1, (4), pp. 353-360
- 20 Gesta, S., Tseng, Y.H., and Kahn, C.R.: 'Developmental origin of fat: Tracking obesity to its source', *Cell*, 2007, 131, (2), pp. 242-256
- 21 Wang, W., and Seale, P.: 'Control of brown and beige fat development', *Nature reviews. Molecular cell biology*, 2016
- 22 Harms, M., and Seale, P.: 'Brown and beige fat: development, function and therapeutic potential', *Nature medicine*, 2013, 19, (10), pp. 1252-1263
- 23 Kim, S.H., and Plutzky, J.: 'Brown Fat and Browning for the Treatment of Obesity and Related Metabolic Disorders', *Diabetes & metabolism journal*, 2016, 40, (1), pp. 12-21
- 24 Cypess, A.M., Lehman, S., Williams, G., Tal, I., Rodman, D., Goldfine, A.B., Kuo, F.C., Palmer, E.L., Tseng, Y., Doria, A., Kolodny, G.M., and Kahn, C.R.: 'Identification and Importance of Brown Adipose Tissue in Adult Humans.', *New Engl J Med*, 2009, 360, (15), pp. 1509-1517
- 25 Saito, M., Okamatsu-Ogura, Y., Matsushita, M., Watanabe, K., Yoneshiro, T., Nio-Kobayashi, J., Iwanaga, T., Miyagawa, M., Kameya, T., Nakada, K., Kawai, Y., and Tsujisaki, M.: 'High Incidence of Metabolically Active Brown Adipose Tissue in Healthy Adult Humans Effects of Cold Exposure and Adiposity', *Diabetes*, 2009, 58, (7), pp. 1526-1531
- 26 Lichtenbelt, W.D.V., Vanhommel, J.W., Smulders, N.M., Drossaerts, J.M.A.F.L., Kemerink, G.J., Bouvy, N.D., Schrauwen, P., and Teule, G.J.J.: 'Cold-Activated Brown Adipose Tissue in Healthy Men.', *New Engl J Med*, 2009, 360, (15), pp. 1500-1508
- 27 Virtanen, K.A., Lidell, M.E., Orava, J., Heglind, M., Westergren, R., Niemi, T., Taittonen, M., Laine, J., Savisto, N.J., Enerback, S., and Nuutila, P.: 'Functional Brown Adipose Tissue in Healthy Adults (vol 360, pg 1518, 2009)', *New Engl J Med*, 2009, 361, (11), pp. 1123-1123
- 28 Nedergaard, J., Bengtsson, T., and Cannon, B.: 'Unexpected evidence for active brown adipose tissue in adult humans', *Am J Physiol-Endoc M*, 2007, 293, (2), pp. E444-E452
- 29 Cypess, A.M., Lehman, S., Williams, G., Tal, I., Rodman, D., Goldfine, A.B., Kuo, F.C., Palmer, E.L., Tseng, Y.H., Doria, A., Kolodny, G.M., and Kahn, C.R.: 'Identification and importance of brown adipose tissue in adult humans', *N Engl J Med*, 2009, 360, (15), pp. 1509-1517

- 30 Bartelt, A., and Heeren, J.: 'Adipose tissue browning and metabolic health', *Nature reviews. Endocrinology*, 2014, 10, (1), pp. 24-36
- 31 Chawla, A., Nguyen, K.D., and Goh, Y.P.: 'Macrophage-mediated inflammation in metabolic disease', *Nat Rev Immunol*, 2011, 11, (11), pp. 738-749
- 32 Wu, D., Molofsky, A.B., Liang, H.E., Ricardo-Gonzalez, R.R., Jouihan, H.A., Bando, J.K., Chawla, A., and Locksley, R.M.: 'Eosinophils sustain adipose alternatively activated macrophages associated with glucose homeostasis', *Science*, 2011, 332, (6026), pp. 243-247
- 33 Qiu, Y., Nguyen, K.D., Odegaard, J.I., Cui, X., Tian, X., Locksley, R.M., Palmiter, R.D., and Chawla, A.: 'Eosinophils and type 2 cytokine signaling in macrophages orchestrate development of functional beige fat', *Cell*, 2014, 157, (6), pp. 1292-1308
- 34 Medrikova, D., Sijmonsma, T.P., Sowodniok, K., Richards, D.M., Delacher, M., Sticht, C., Gretz, N., Schafmeier, T., Feuerer, M., and Herzig, S.: 'Brown adipose tissue harbors a distinct sub-population of regulatory T cells', *PLoS One*, 2015, 10, (2), pp. e0118534
- 35 Sun, S., Ji, Y., Kersten, S., and Qi, L.: 'Mechanisms of inflammatory responses in obese adipose tissue', *Annual review of nutrition*, 2012, 32, pp. 261-286
- 36 Choe, S.S., Huh, J.Y., Hwang, I.J., Kim, J.I., and Kim, J.B.: 'Adipose Tissue Remodeling: its Role in energy Metabolism and Metabolic Disorders', *Frontiers in endocrinology*, 2016, 7
- 37 Wensveen, F.M., Valentic, S., Sestan, M., Wensveen, T.T., and Polic, B.: 'The "Big Bang" in obese fat: Events initiating obesity-induced adipose tissue inflammation', *Eur J Immunol*, 2015, 45, (9), pp. 2446-2456
- 38 Italiani, P., and Boraschi, D.: 'From monocytes to M1/M2 macrophages: phenotypical vs. functional differentiation', *Front Immunol*, 2014, 5
- 39 Weisberg, S.P., McCann, D., Desai, M., Rosenbaum, M., Leibel, R.L., and Ferrante, A.W.: 'Obesity is associated with macrophage accumulation in adipose tissue', *Journal of Clinical Investigation*, 2003, 112, (12), pp. 1796-1808
- 40 Lumeng, C.N., Deyoung, S.M., Bodzin, J.L., and Saltiel, A.R.: 'Increased inflammatory properties of adipose tissue macrophages recruited during diet-induced obesity', *Diabetes*, 2007, 56, (1), pp. 16-23
- 41 Lumeng, C.N., Bodzin, J.L., and Saltiel, A.R.: 'Obesity induces a phenotypic switch in adipose tissue macrophage polarization', *The Journal of clinical investigation*, 2007, 117, (1), pp. 175-184
- 42 Lumeng, C.N., Bodzin, J.L., and Saltiel, A.R.: 'Obesity induces a phenotypic switch in adipose tissue macrophage polarization', *Journal of Clinical Investigation*, 2007, 117, (1), pp. 175-184

- 43 Negrin, K.A., Flach, R.J.R., DiStefano, M.T., Matevossian, A., Friedline, R.H., Jung, D., Kim, J.K., and Czech, M.P.: 'IL-1 Signaling in Obesity-Induced Hepatic Lipogenesis and Steatosis', *PLoS One*, 2014, 9, (9)
- 44 Thaler, J.P., Yi, C.X., Schur, E.A., Guyenet, S.J., Hwang, B.H., Dietrich, M.O., Zhao, X., Sarruf, D.A., Izgur, V., Maravilla, K.R., Nguyen, H.T., Fischer, J.D., Matsen, M.E., Wisse, B.E., Morton, G.J., Horvath, T.L., Baskin, D.G., Tschop, M.H., and Schwartz, M.W.: 'Obesity is associated with hypothalamic injury in rodents and humans', *The Journal of clinical investigation*, 2012, 122, (1), pp. 153-162
- 45 Xu, H., Barnes, G.T., Yang, Q., Tan, G., Yang, D., Chou, C.J., Sole, J., Nichols, A., Ross, J.S., Tartaglia, L.A., and Chen, H.: 'Chronic inflammation in fat plays a crucial role in the development of obesity-related insulin resistance', *The Journal of clinical investigation*, 2003, 112, (12), pp. 1821-1830
- 46 Bachelier, F., Ben-Baruch, A., Burkhardt, A.M., Combadiere, C., Farber, J.M., Graham, G.J., Horuk, R., Sparre-Ulrich, A.H., Locati, M., Luster, A.D., Mantovani, A., Matsushima, K., Murphy, P.M., Nibbs, R., Nomiyama, H., Power, C.A., Proudfoot, A.E., Rosenkilde, M.M., Rot, A., Sozzani, S., Thelen, M., Yoshie, O., and Zlotnik, A.: 'International Union of Basic and Clinical Pharmacology. [corrected]. LXXXIX. Update on the extended family of chemokine receptors and introducing a new nomenclature for atypical chemokine receptors', *Pharmacological reviews*, 2014, 66, (1), pp. 1-79
- 47 Mantovani, A., Bonecchi, R., and Locati, M.: 'Tuning inflammation and immunity by chemokine sequestration: decoys and more', *Nature reviews. Immunology*, 2006, 6, (12), pp. 907-918
- 48 Blanchet, X., Langer, M., Weber, C., Koenen, R.R., and von Hundelshausen, P.: 'Touch of chemokines', *Front Immunol*, 2012, 3, pp. 175
- 49 Bryant, V.L., and Slade, C.A.: 'Chemokines, their receptors and human disease: the good, the bad and the itchy', *Immunol Cell Biol*, 2015, 93, (4), pp. 364-371
- 50 Jung, U.J., and Choi, M.S.: 'Obesity and Its Metabolic Complications: The Role of Adipokines and the Relationship between Obesity, Inflammation, Insulin Resistance, Dyslipidemia and Nonalcoholic Fatty Liver Disease', *Int J Mol Sci*, 2014, 15, (4), pp. 6184-6223
- 51 Panee, J.: 'Monocyte Chemoattractant Protein 1 (MCP-1) in obesity and diabetes', *Cytokine*, 2012, 60, (1), pp. 1-12
- 52 Nara, N., Nakayama, Y., Okamoto, S., Tamura, H., Kiyono, M., Muraoka, M., Tanaka, K., Taya, C., Shitara, H., Ishii, R., Yonekawa, H., Minokoshi, Y., and Hara, T.: 'Disruption of CXC motif chemokine ligand-14 in mice ameliorates obesity-induced insulin resistance', *J Biol Chem*, 2007, 282, (42), pp. 30794-30803

- 53 Keophiphath, M., Rouault, C., Divoux, A., Clement, K., and Lacasa, D.: 'CCL5 Promotes Macrophage Recruitment and Survival in Human Adipose Tissue', *Arterioscl Throm Vas*, 2010, 30, (1), pp. 39-U113
- 54 Chavey, C., Lazenne, G., Lagarrigue, S., Clape, C., Iankova, I., Teyssier, J., Annicotte, J.S., Schmidt, J., Matak, C., Yamamoto, H., Sanches, R., Guma, A., Stich, V., Vitkova, M., Jardin-Watelet, B., Renard, E., Strieter, R., Tuthill, A., Hotamisligil, G.S., Vidal-Puig, A., Zorzano, A., Langin, D., and Fajas, L.: 'CXC Ligand 5 Is an Adipose-Tissue Derived Factor that Links Obesity to Insulin Resistance', *Cell metabolism*, 2009, 9, (4), pp. 339-349
- 55 Huber, J., Kiefer, F.W., Zeyda, M., Ludvik, B., Silberhumer, G.R., Prager, G., Zlabinger, G.J., and Stulnig, T.M.: 'CC chemokine and CC chemokine receptor profiles in visceral and subcutaneous adipose tissue are altered in human obesity', *J Clin Endocr Metab*, 2008, 93, (8), pp. 3215-3221
- 56 Shah, R., Hinkle, C.C., Ferguson, J.F., Mehta, N.N., Li, M., Qu, L., Lu, Y., Putt, M.E., Ahima, R.S., and Reilly, M.P.: 'Fractalkine is a novel human adipochemokine associated with type 2 diabetes', *Diabetes*, 2011, 60, (5), pp. 1512-1518
- 57 Rostene, W., Kitabgi, P., and Parsadaniantz, S.M.: 'Chemokines: a new class of neuromodulator?', *Nature reviews. Neuroscience*, 2007, 8, (11), pp. 895-903
- 58 Pan, Y., Lloyd, C., Zhou, H., Dolich, S., Deeds, J., Gonzalo, J.A., Vath, J., Gosselin, M., Ma, J., Dussault, B., Woolf, E., Alperin, G., Culpepper, J., Gutierrez-Ramos, J.C., and Gearing, D.: 'Neurotactin, a membrane-anchored chemokine upregulated in brain inflammation', *Nature*, 1997, 387, (6633), pp. 611-617
- 59 Bazan, J.F., Bacon, K.B., Hardiman, G., Wang, W., Soo, K., Rossi, D., Greaves, D.R., Zlotnik, A., and Schall, T.J.: 'A new class of membrane-bound chemokine with a CX3C motif', *Nature*, 1997, 385, (6617), pp. 640-644
- 60 <http://www.ncbi.nlm.nih.gov/protein/4506857?report=genpept>
- 61 <http://www.ncbi.nlm.nih.gov/protein/31982017?report=genpept>
- 62 Wojdasiewicz, P., Poniatowski, L.A., Kotela, A., Deszczynski, J., Kotela, I., and Szukiewicz, D.: 'The Chemokine CX3CL1 (Fractalkine) and its Receptor CX3CR1: Occurrence and Potential Role in Osteoarthritis', *Arch Immunol Ther Ex*, 2014, 62, (5), pp. 395-403
- 63 Hundhausen, C., Schulte, A., Schulz, B., Andrzejewski, M.G., Schwarz, N., von Hundelshausen, P., Winter, U., Paliga, K., Reiss, K., Saftig, P., Weber, C., and Ludwig, A.: 'Regulated shedding of transmembrane chemokines by the disintegrin and metalloproteinase 10 facilitates detachment of adherent leukocytes', *J Immunol*, 2007, 178, (12), pp. 8064-8072
- 64 Menghini, R., Fiorentino, L., Casagrande, V., Lauro, R., and Federici, M.: 'The role of ADAM17 in metabolic inflammation', *Atherosclerosis*, 2013, 228, (1), pp. 12-17

- 65 de Meijer, V.E., Sverdlov, D.Y., Le, H.D., Popov, Y., and Puder, M.: 'Tissue-specific differences in inflammatory infiltrate and matrix metalloproteinase expression in adipose tissue and liver of mice with diet-induced obesity', *Hepatology research : the official journal of the Japan Society of Hepatology*, 2012, 42, (6), pp. 601-610
- 66 Voros, G., Maquoi, E., Collen, D., and Lijnen, H.R.: 'Differential expression of plasminogen activator inhibitor-1, tumor necrosis factor-alpha, TNF-alpha converting enzyme and ADAMTS family members in murine fat territories', *Biochimica et biophysica acta*, 2003, 1625, (1), pp. 36-42
- 67 Kim, K.W., Vallon-Eberhard, A., Zigmond, E., Farache, J., Shezen, E., Shakhar, G., Ludwig, A., Lira, S.A., and Jung, S.: 'In vivo structure/function and expression analysis of the CX3C chemokine fractalkine', *Blood*, 2011, 118, (22), pp. E156-E167
- 68 Lucas, A.D., Chadwick, N., Warren, B.F., Jewell, D.P., Gordon, S., Powrie, F., and Greaves, D.R.: 'The transmembrane form of the CX3CL1 chemokine fractalkine is expressed predominantly by epithelial cells in vivo', *American Journal of Pathology*, 2001, 158, (3), pp. 855-866
- 69 Efsen, E., Grappone, C., DeFranco, R.M., Milani, S., Romanelli, R.G., Bonacchi, A., Caligiuri, A., Failli, P., Annunziato, F., Pagliai, G., Pinzani, M., Laffi, G., Gentilini, P., and Marra, F.: 'Up-regulated expression of fractalkine and its receptor CX3CR1 during liver injury in humans', *Journal of hepatology*, 2002, 37, (1), pp. 39-47
- 70 Ludwig, A., Berkhout, T., Moores, K., Groot, P., and Chapman, G.: 'Fractalkine is expressed by smooth muscle cells in response to IFN-gamma and TNF-alpha and is modulated by metalloproteinase activity', *Journal of Immunology*, 2002, 168, (2), pp. 604-612
- 71 Butoi, E.D., Gan, A.M., Manduteanu, I., Stan, D., Calin, M., Pirvulescu, M., Koenen, R.R., Weber, C., and Simionescu, M.: 'Cross talk between smooth muscle cells and monocytes/activated monocytes via CX3CL1/CX3CR1 axis augments expression of pro-atherogenic molecules', *Bba-Mol Cell Res*, 2011, 1813, (12), pp. 2026-2035
- 72 Jung, S., Aliberti, J., Graemmel, P., Sunshine, M.J., Kreutzberg, G.W., Sher, A., and Littman, D.R.: 'Analysis of fractalkine receptor CX(3)CR1 function by targeted deletion and green fluorescent protein reporter gene insertion', *Mol Cell Biol*, 2000, 20, (11), pp. 4106-4114
- 73 Morris, D.L., Oatmen, K.E., Wang, T., DelProposto, J.L., and Lumeng, C.N.: 'CX3CR1 deficiency does not influence trafficking of adipose tissue macrophages in mice with diet-induced obesity', *Obesity (Silver Spring)*, 2012, 20, (6), pp. 1189-1199
- 74 Wojdasiewicz, P., Poniatowski, L.A., Kotela, A., Deszczynski, J., Kotela, I., and Szukiewicz, D.: 'The chemokine CX3CL1 (fractalkine) and its receptor CX3CR1: occurrence and potential role in osteoarthritis', *Arch Immunol Ther Exp (Warsz)*, 2014, 62, (5), pp. 395-403

- 75 Al-Aoukaty, A., Rolstad, B., Giaid, A., and Maghazachi, A.A.: 'MIP-3alpha, MIP-3beta and fractalkine induce the locomotion and the mobilization of intracellular calcium, and activate the heterotrimeric G proteins in human natural killer cells', *Immunology*, 1998, 95, (4), pp. 618-624
- 76 Cotter, R., Williams, C., Ryan, L., Erichsen, D., Lopez, A., Peng, H., and Zheng, J.: 'Fractalkine (CX3CL1) and brain inflammation: Implications for HIV-1-associated dementia', *Journal of neurovirology*, 2002, 8, (6), pp. 585-598
- 77 Sheridan, G.K., and Murphy, K.J.: 'Neuron-glia crosstalk in health and disease: fractalkine and CX3CR1 take centre stage', *Open biology*, 2013, 3, (12), pp. 130181
- 78 Lyons, A., Lynch, A.M., Downer, E.J., Hanley, R., O'Sullivan, J.B., Smith, A., and Lynch, M.A.: 'Fractalkine-induced activation of the phosphatidylinositol-3 kinase pathway attenuates microglial activation in vivo and in vitro', *Journal of neurochemistry*, 2009, 110, (5), pp. 1547-1556
- 79 Sun, J.L., Xiao, C., Lu, B., Zhang, J., Yuan, X.Z., Chen, W., Yu, L.N., Zhang, F.J., Chen, G., and Yan, M.: 'CX3CL1/CX3CR1 regulates nerve injury-induced pain hypersensitivity through the ERK5 signaling pathway', *Journal of neuroscience research*, 2013, 91, (4), pp. 545-553
- 80 White, G.E., and Greaves, D.R.: 'Fractalkine: a survivor's guide: chemokines as antiapoptotic mediators', *Arteriosclerosis, thrombosis, and vascular biology*, 2012, 32, (3), pp. 589-594
- 81 Umehara, H., Bloom, E.T., Okazaki, T., Nagano, Y., Yoshie, O., and Imai, T.: 'Fractalkine in vascular biology: from basic research to clinical disease', *Arteriosclerosis, thrombosis, and vascular biology*, 2004, 24, (1), pp. 34-40
- 82 Jones, B.A., Beamer, M., and Ahmed, S.: 'Fractalkine/CX3CL1: A Potential New Target for Inflammatory Diseases', *Mol Interv*, 2010, 10, (5), pp. 263-270
- 83 Jung, S., Aliberti, J., Graemmel, P., Sunshine, M.J., Kreutzberg, G.W., Sher, A., and Littman, D.R.: 'Analysis of fractalkine receptor CX(3)CR1 function by targeted deletion and green fluorescent protein reporter gene insertion', *Mol Cell Biol*, 2000, 20, (11), pp. 4106-4114
- 84 Collins, S., Martin, T.L., Surwit, R.S., and Robidoux, J.: 'Genetic vulnerability to diet-induced obesity in the C57BL/6J mouse: physiological and molecular characteristics', *Physiology & behavior*, 2004, 81, (2), pp. 243-248
- 85 Kovacs, K.J., and Makara, G.B.: 'Corticosterone and dexamethasone act at different brain sites to inhibit adrenalectomy-induced adrenocorticotropin hypersecretion', *Brain research*, 1988, 474, (2), pp. 205-210

- 86 Zelena, D., Foldes, A., Mergl, Z., Barna, I., Kovacs, K.J., and Makara, G.B.: 'Effects of repeated restraint stress on hypothalamo-pituitary-adrenocortical function in vasopressin deficient Brattleboro rats', *Brain research bulletin*, 2004, 63, (6), pp. 521-530
- 87 Nakamura, Y., Sato, T., Shiimura, Y., Miura, Y., and Kojima, M.: 'FABP3 and brown adipocyte-characteristic mitochondrial fatty acid oxidation enzymes are induced in beige cells in a different pathway from UCP1', *Biochem Biophys Res Commun*, 2013, 441, (1), pp. 42-46
- 88 Samaan, M.C.: 'The macrophage at the intersection of immunity and metabolism in obesity', *Diabetol Metab Syndr*, 2011, 3
- 89 Cinti, S., Mitchell, G., Barbatelli, G., Murano, I., Ceresi, E., Faloia, E., Wang, S.P., Fortier, M., Greenberg, A.S., and Obin, M.S.: 'Adipocyte death defines macrophage localization and function in adipose tissue of obese mice and humans', *J Lipid Res*, 2005, 46, (11), pp. 2347-2355
- 90 Nguyen, K.D., Qiu, Y., Cui, X., Goh, Y.P., Mwangi, J., David, T., Mukundan, L., Brombacher, F., Locksley, R.M., and Chawla, A.: 'Alternatively activated macrophages produce catecholamines to sustain adaptive thermogenesis', *Nature*, 2011, 480, (7375), pp. 104-108
- 91 Hariri, N., and Thibault, L.: 'High-fat diet-induced obesity in animal models', *Nutrition research reviews*, 2010, 23, (2), pp. 270-299
- 92 Pecoraro, N., Reyes, F., Gomez, F., Bhargava, A., and Dallman, M.F.: 'Chronic stress promotes palatable feeding, which reduces signs of stress: feedforward and feedback effects of chronic stress', *Endocrinology*, 2004, 145, (8), pp. 3754-3762
- 93 Foster, M.T., Warne, J.P., Ginsberg, A.B., Horneman, H.F., Pecoraro, N.C., Akana, S.F., and Dallman, M.F.: 'Palatable foods, stress, and energy stores sculpt corticotropin-releasing factor, adrenocorticotropin, and corticosterone concentrations after restraint', *Endocrinology*, 2009, 150, (5), pp. 2325-2333
- 94 Hariri, N., Gougeon, R., and Thibault, L.: 'A highly saturated fat-rich diet is more obesogenic than diets with lower saturated fat content', *Nutrition research*, 2010, 30, (9), pp. 632-643
- 95 Sampey, B.P., Vanhoose, A.M., Winfield, H.M., Freerman, A.J., Muehlbauer, M.J., Fueger, P.T., Newgard, C.B., and Makowski, L.: 'Cafeteria diet is a robust model of human metabolic syndrome with liver and adipose inflammation: comparison to high-fat diet', *Obesity*, 2011, 19, (6), pp. 1109-1117
- 96 Tabbi-Anneni, I., Cooksey, R., Gunda, V., Liu, S., Mueller, A., Song, G., McClain, D.A., and Wang, L.: 'Overexpression of nuclear receptor SHP in adipose tissues affects diet-induced obesity and adaptive thermogenesis', *American journal of physiology. Endocrinology and metabolism*, 2010, 298, (5), pp. E961-970

- 97 Maimaitiyiming, H., Norman, H., Zhou, Q., and Wang, S.: 'CD47 deficiency protects mice from diet-induced obesity and improves whole body glucose tolerance and insulin sensitivity', *Scientific reports*, 2015, 5, pp. 8846
- 98 Kus, V., Prazak, T., Brauner, P., Hensler, M., Kuda, O., Flachs, P., Janovska, P., Medrikova, D., Rossmeisl, M., Jilkova, Z., Stefl, B., Pastalkova, E., Drahotka, Z., Houstek, J., and Kopecky, J.: 'Induction of muscle thermogenesis by high-fat diet in mice: association with obesity-resistance', *American journal of physiology. Endocrinology and metabolism*, 2008, 295, (2), pp. E356-367
- 99 Williams, L.M., Campbell, F.M., Drew, J.E., Koch, C., Hoggard, N., Rees, W.D., Kamolrat, T., Thi Ngo, H., Steffensen, I.L., Gray, S.R., and Tups, A.: 'The development of diet-induced obesity and glucose intolerance in C57BL/6 mice on a high-fat diet consists of distinct phases', *PLoS One*, 2014, 9, (8), pp. e106159
- 100 Lin, S., Thomas, T.C., Storlien, L.H., and Huang, X.F.: 'Development of high fat diet-induced obesity and leptin resistance in C57Bl/6J mice', *International journal of obesity and related metabolic disorders : journal of the International Association for the Study of Obesity*, 2000, 24, (5), pp. 639-646
- 101 Lee, Y.S., Morinaga, H., Kim, J.J., Lagakos, W., Taylor, S., Keshwani, M., Perkins, G., Dong, H., Kayali, A.G., Sweet, I.R., and Olefsky, J.: 'The fractalkine/CX3CR1 system regulates beta cell function and insulin secretion', *Cell*, 2013, 153, (2), pp. 413-425
- 102 Shah, R., O'Neill, S.M., Hinkle, C., Caughey, J., Stephan, S., Lynch, E., Bermingham, K., Lynch, G., Ahima, R.S., and Reilly, M.P.: 'Metabolic Effects of CX3CR1 Deficiency in Diet-Induced Obese Mice', *PLoS One*, 2015, 10, (9), pp. e0138317
- 103 Rosenbaum, M., Knight, R., and Leibel, R.L.: 'The gut microbiota in human energy homeostasis and obesity', *Trends in endocrinology and metabolism: TEM*, 2015, 26, (9), pp. 493-501
- 104 Cani, P.D., Bibiloni, R., Knauf, C., Waget, A., Neyrinck, A.M., Delzenne, N.M., and Burcelin, R.: 'Changes in gut microbiota control metabolic endotoxemia-induced inflammation in high-fat diet-induced obesity and diabetes in mice', *Diabetes*, 2008, 57, (6), pp. 1470-1481
- 105 Fei, N., and Zhao, L.: 'An opportunistic pathogen isolated from the gut of an obese human causes obesity in germfree mice', *The ISME journal*, 2013, 7, (4), pp. 880-884
- 106 Muller, V.M., Zietek, T., Rohm, F., Fiamoncini, J., Lagkouvardos, I., Haller, D., Clavel, T., and Daniel, H.: 'Gut barrier impairment by high-fat diet in mice depends on housing conditions', *Molecular nutrition & food research*, 2016, 60, (4), pp. 897-908
- 107 Dallman, M.F., Pecoraro, N., Akana, S.F., La Fleur, S.E., Gomez, F., Houshyar, H., Bell, M.E., Bhatnagar, S., Laugero, K.D., and Manalo, S.: 'Chronic stress and obesity: a new

view of "comfort food", *Proceedings of the National Academy of Sciences of the United States of America*, 2003, 100, (20), pp. 11696-11701

108 Auvinen, H.E., Romijn, J.A., Biermasz, N.R., Havekes, L.M., Smit, J.W., Rensen, P.C., and Pereira, A.M.: 'Effects of high fat diet on the Basal activity of the hypothalamus-pituitary-adrenal axis in mice: a systematic review', *Horm Metab Res*, 2011, 43, (13), pp. 899-906

109 Kershaw, E.E., Morton, N.M., Dhillon, H., Ramage, L., Seckl, J.R., and Flier, J.S.: 'Adipocyte-specific glucocorticoid inactivation protects against diet-induced obesity', *Diabetes*, 2005, 54, (4), pp. 1023-1031

110 Man, T.Y., Michailidou, Z., Gokcel, A., Ramage, L., Chapman, K.E., Kenyon, C.J., Seckl, J.R., and Morton, N.M.: 'Dietary manipulation reveals an unexpected inverse relationship between fat mass and adipose 11beta-hydroxysteroid dehydrogenase type 1', *American journal of physiology. Endocrinology and metabolism*, 2011, 300, (6), pp. E1076-1084

111 Cooper, M.S., and Stewart, P.M.: '11Beta-hydroxysteroid dehydrogenase type 1 and its role in the hypothalamus-pituitary-adrenal axis, metabolic syndrome, and inflammation', *The Journal of clinical endocrinology and metabolism*, 2009, 94, (12), pp. 4645-4654

112 Rosenwald, M., Perdikari, A., Rulicke, T., and Wolfrum, C.: 'Bi-directional interconversion of brite and white adipocytes', *Nat Cell Biol*, 2013, 15, (6), pp. 659-667

113 Rosenwald, M., and Wolfrum, C.: 'The origin and definition of brite versus white and classical brown adipocytes', *Adipocyte*, 2014, 3, (1), pp. 4-9

114 Fitzgibbons, T.P., Kogan, S., Aouadi, M., Hendricks, G.M., Straubhaar, J., and Czech, M.P.: 'Similarity of mouse perivascular and brown adipose tissues and their resistance to diet-induced inflammation', *Am J Physiol Heart Circ Physiol*, 2011, 301, (4), pp. H1425-1437

115 Gao, M., Ma, Y., and Liu, D.: 'High-fat diet-induced adiposity, adipose inflammation, hepatic steatosis and hyperinsulinemia in outbred CD-1 mice', *PLoS One*, 2015, 10, (3), pp. e0119784

116 Altintas, M.M., Azad, A., Nayer, B., Contreras, G., Zaias, J., Faul, C., Reiser, J., and Nayer, A.: 'Mast cells, macrophages, and crown-like structures distinguish subcutaneous from visceral fat in mice', *J Lipid Res*, 2011, 52, (3), pp. 480-488

117 Weisberg, S.P., McCann, D., Desai, M., Rosenbaum, M., Leibel, R.L., and Ferrante, A.W., Jr.: 'Obesity is associated with macrophage accumulation in adipose tissue', *J Clin Invest*, 2003, 112, (12), pp. 1796-1808

118 Hageman, R.S., Wagener, A., Hantschel, C., Svenson, K.L., Churchill, G.A., and Brockmann, G.A.: 'High-fat diet leads to tissue-specific changes reflecting risk factors for diseases in DBA/2J mice', *Physiol Genomics*, 2010, 42, (1), pp. 55-66

- 119 Herrero, L., Shapiro, H., Nayer, A., Lee, J., and Shoelson, S.E.: 'Inflammation and adipose tissue macrophages in lipodystrophic mice', *Proc Natl Acad Sci U S A*, 2010, 107, (1), pp. 240-245
- 120 Bao, B., Chen, Y.G., Zhang, L., Na Xu, Y.L., Wang, X., Liu, J., and Qu, W.: 'Momordica charantia (Bitter Melon) reduces obesity-associated macrophage and mast cell infiltration as well as inflammatory cytokine expression in adipose tissues', *PLoS One*, 2013, 8, (12), pp. e84075
- 121 Lee, B.C., and Lee, J.: 'Cellular and molecular players in adipose tissue inflammation in the development of obesity-induced insulin resistance', *Biochimica et biophysica acta*, 2014, 1842, (3), pp. 446-462
- 122 Hill, B.G.: 'Insights into an adipocyte whitening program', *Adipocyte*, 2015, 4, (1), pp. 75-80
- 123 Lumeng, C.N., and Saltiel, A.R.: 'Inflammatory links between obesity and metabolic disease', *J Clin Invest*, 2011, 121, (6), pp. 2111-2117
- 124 Chen, A., Mumick, S., Zhang, C., Lamb, J., Dai, H., Weingarh, D., Mudgett, J., Chen, H., MacNeil, D.J., Reitman, M.L., and Qian, S.: 'Diet induction of monocyte chemoattractant protein-1 and its impact on obesity', *Obes Res*, 2005, 13, (8), pp. 1311-1320
- 125 Lesnik, P., Haskell, C.A., and Charo, I.F.: 'Decreased atherosclerosis in CX3CR1^{-/-} mice reveals a role for fractalkine in atherogenesis', *J Clin Invest*, 2003, 111, (3), pp. 333-340
- 126 Liu, P., Yu, Y.R., Spencer, J.A., Johnson, A.E., Vallanat, C.T., Fong, A.M., Patterson, C., and Patel, D.D.: 'CX3CR1 deficiency impairs dendritic cell accumulation in arterial intima and reduces atherosclerotic burden', *Arterioscler Thromb Vasc Biol*, 2008, 28, (2), pp. 243-250
- 127 Saederup, N., Chan, L., Lira, S.A., and Charo, I.F.: 'Fractalkine deficiency markedly reduces macrophage accumulation and atherosclerotic lesion formation in CCR2^{-/-} mice: evidence for independent chemokine functions in atherogenesis', *Circulation*, 2008, 117, (13), pp. 1642-1648
- 128 Stienstra, R., van Diepen, J.A., Tack, C.J., Zaki, M.H., van de Veerdonk, F.L., Perera, D., Neale, G.A., Hooiveld, G.J., Hijmans, A., Vroegrijk, I., van den Berg, S., Romijn, J., Rensen, P.C., Joosten, L.A., Netea, M.G., and Kanneganti, T.D.: 'Inflammasome is a central player in the induction of obesity and insulin resistance', *Proceedings of the National Academy of Sciences of the United States of America*, 108, (37), pp. 15324-15329
- 129 Vandanmagsar, B., Youm, Y.H., Ravussin, A., Galgani, J.E., Stadler, K., Mynatt, R.L., Ravussin, E., Stephens, J.M., and Dixit, V.D.: 'The NLRP3 inflammasome instigates obesity-induced inflammation and insulin resistance', *Nature medicine*, 2011, 17, (2), pp. 179-188

- 130 Tacke, F., Alvarez, D., Kaplan, T.J., Jakubzick, C., Spanbroek, R., Llodra, J., Garin, A., Liu, J., Mack, M., van Rooijen, N., Lira, S.A., Habenicht, A.J., and Randolph, G.J.: 'Monocyte subsets differentially employ CCR2, CCR5, and CX3CR1 to accumulate within atherosclerotic plaques', *The Journal of clinical investigation*, 2007, 117, (1), pp. 185-194
- 131 Juge-Aubry, C.E., Somm, E., Pernin, A., Alizadeh, N., Giusti, V., Dayer, J.M., and Meier, C.A.: 'Adipose tissue is a regulated source of interleukin-10', *Cytokine*, 2005, 29, (6), pp. 270-274
- 132 Stienstra, R., Duval, C., Keshtkar, S., van der Laak, J., Kersten, S., and Muller, M.: 'Peroxisome proliferator-activated receptor gamma activation promotes infiltration of alternatively activated macrophages into adipose tissue', *The Journal of biological chemistry*, 2008, 283, (33), pp. 22620-22627
- 133 Nisoli, E., Briscini, L., Giordano, A., Tonello, C., Wiesbrock, S.M., Uysal, K.T., Cinti, S., Carruba, M.O., and Hotamisligil, G.S.: 'Tumor necrosis factor alpha mediates apoptosis of brown adipocytes and defective brown adipocyte function in obesity', *Proc Natl Acad Sci U S A*, 2000, 97, (14), pp. 8033-8038
- 134 Kralisch, S., Klein, J., Lossner, U., Bluher, M., Paschke, R., Stumvoll, M., and Fasshauer, M.: 'Isoproterenol, TNFalpha, and insulin downregulate adipose triglyceride lipase in 3T3-L1 adipocytes', *Mol Cell Endocrinol*, 2005, 240, (1-2), pp. 43-49
- 135 Sakamoto, T., Takahashi, N., Sawaragi, Y., Naknukool, S., Yu, R., Goto, T., and Kawada, T.: 'Inflammation induced by RAW macrophages suppresses UCP1 mRNA induction via ERK activation in 10T1/2 adipocytes', *Am J Physiol Cell Physiol*, 2013, 304, (8), pp. C729-738
- 136 Sakamoto, T., Nitta, T., Maruno, K., Yeh, Y.S., Kuwata, H., Tomita, K., Goto, T., Takahashi, N., and Kawada, T.: 'Macrophage infiltration into obese adipose tissues suppresses the induction of UCP1 expression in mice', *American journal of physiology. Endocrinology and metabolism*, 2016, pp. ajpendo 00028 02015
- 137 Denes, A., Drake, C., Stordy, J., Chamberlain, J., McColl, B.W., Gram, H., Crossman, D., Francis, S., Allan, S.M., and Rothwell, N.J.: 'Interleukin-1 mediates neuroinflammatory changes associated with diet-induced atherosclerosis', *Journal of the American Heart Association*, 2012, 1, (3), pp. e002006
- 138 Morrison, C.D., Morton, G.J., Niswender, K.D., Gelling, R.W., and Schwartz, M.W.: 'Leptin inhibits hypothalamic Npy and Agrp gene expression via a mechanism that requires phosphatidylinositol 3-OH-kinase signaling', *Am J Physiol-Endoc M*, 2005, 289, (6), pp. E1051-E1057
- 139 Schwartz, M.W., Sipols, A.J., Marks, J.L., Sanacora, G., White, J.D., Scheurink, A., Kahn, S.E., Baskin, D.G., Woods, S.C., Figlewicz, D.P., and Porte, D.: 'Inhibition of

Hypothalamic Neuropeptide-Y Gene-Expression by Insulin', *Endocrinology*, 1992, 130, (6), pp. 3608-3616

140 Sato, I., Arima, H., Ozaki, N., Watanabe, M., Goto, M., Hayashi, M., Banno, R., Nagasaki, H., and Oiso, Y.: 'Insulin inhibits neuropeptide Y gene expression in the arcuate nucleus through GABAergic systems', *J Neurosci*, 2005, 25, (38), pp. 8657-8664

141 Poupel, L., Boissonnas, A., Hermand, P., Dorgham, K., Guyon, E., Auvynet, C., Saint Charles, F., Lesnik, P., Deterre, P., and Combadiere, C.: 'Pharmacological Inhibition of the Chemokine Receptor, CX3CR1, Reduces Atherosclerosis in Mice', *Arterioscl Throm Vas*, 2013, 33, (10), pp. 2297-2305